UNIVERSITY OF SURREY

Faculty of Engineering and Physical Sciences

Civil & Environmental Engineering

Title: Soil-structure interaction modelling on the seismic performance of a continuous span bridge – a cost-benefit analysis

Author's Name: Wazeer Ali

Supervisor: Dr. Helder de Sousa

Co-Supervisor: Professor Subhamoy Bhattacharya

A dissertation submitted in partial fulfilment of the requirements for the Degree of Master of Science in Civil Engineering

August 2018

Declaration of Originality

I confirm that the dissertation entitled '*Soil-structure interaction modelling on the seismic performance of a continuous span bridge – a cost-benefit analysis*' for the partial fulfilment of the degree of MSc. in Civil Engineering, has been composed by myself and has not been presented or accepted in any previous application for a degree. The work, of which this is a record, has been carried out by myself unless otherwise stated and where the work is mine, it reflects personal views and values. All quotations have been distinguished by quotation marks and all sources of information have been acknowledged by means of references including those of the internet.

Student's name: Wazeer Ali

Date: August 21st, 2018

Acknowledgements

The author wishes to express his sincerest gratitude to Dr Helder de Sousa, who pushed the limits to ensure a fine-quality research and report is produced. He truly is a dedicated and reliable supervisor and a great friend.

Through Dr de Sousa, the author is also very grateful to Dr Paolo Bocchini and Dr Alfred Strauss who provided insightful views and guidance towards the methodologies and assimilating data for the fragility curves.

Professor Bhattacharya also provided assistance where needed for the geotechnical aspects and was always willing to listen.

Last but not least, the author would like to address his wife, Reshma, whose undying love and support fuelled his strength to complete the tasks.

ABSTRACT

According to the current state-of-the-art, the evaluation and assessment of bridge fragility is mainly explored from the point of view of the structure specificities only rather than a more holistic approach where the conditions of the sites where they are located are also included. Hence, the effect of Soil-Structure Interaction (SSI) on the seismic performance of a bridge needs to be properly addressed in the context of fragility, i.e. the probability of damage due to a seismic event. Nevertheless, several SSI methods are available in the literature, which means that, in a first instance, a better understanding on how these approaches influence these bridge fragility curves is highly important and mainly from a cost-benefit basis.

In this context, this report aims to discuss how different SSI affects the structural seismic response of a bridge type widely used in transportation networks – MSC Steel Girder bridge. More specifically, and according to the advancements on the state-of-the-art, three SSI methods are considered, mainly: (i) the Lumped-spring method, (ii) the Winkler-spring method and (iii) the Direct Finite Element method. In addition, two different typical sites are considered, with one of them showing potential of liquefaction. The author believes that with this approach, a robust and credible discussion on the real effect of the SSI is achieved, which is mainly done at two levels: (i) the bridge component and (ii) the bridge system for different levels of damage. Finally, a cost-benefit analysis is promoted with the objective of informing, qualitative and quantitatively, the decision-makers on the best SSI approach depending on the specific requirements established by them.

Based on the results presented in this report, it is concluded that the different SSI methods leads to significant differences mainly on the bridge component fragility, when compared to the bridge system fragility. Moreover, these differences become higher when the in situ conditions of the soil are mechanical weaker, mainly for the scenario of higher levels of damage. Nevertheless, this does not mean that by investing on a refined analysis leads to best outcome on a cost-benefit basis, from the decision-maker point of view. Overall, the Winkler-spring method is found to be the most economical method.

Table of Contents

List of Figures

List of Tables

I. INTRODUCTION

Bridges are perhaps the backbone of transportation networks in a socio-economic context of any country. Their influences include: a better quality of life by enabling cheaper transportation of supplies along easier routes, increased land value and reduced traffic congestion in other roads. Therefore, when bridges fail there can be significant hindrance on the development of an economy.

Bridge failures due to inadequate foundation is a very real issue and two examples are shown in Figure 1. In the Showa Bridge (left) liquefaction caused an increase in the period of the bridge piers (dynamic failure) resulting in unseating of the decks. In the Juan Pablo II Bridge (right), liquefaction also caused pile capacity failure resulting in excessive settlements.

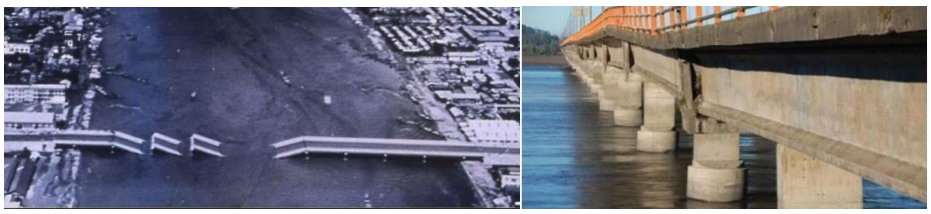

Figure 1: Left-Showa Bridge after 1964 Niigata earthquake (Bhattacharya et al., 2014); Right-Juan Pablo II Bridge after 2010 Chile earthquake (Kawashima et al., 2011)

In seismic areas, bridges management is no trivial task. At both project and network levels, decisions have to be made on the basis of seismic risk assessments and post-earthquake emergency response plans. In the context of funding, prioritising the retrofitting of older bridges, which were built before seismic codes, estimating repair costs are crucial parts of the process.

Options such as multi criteria assessment and statistical data from previous earthquakes can be used to help bridge managers make the above decisions. But the current trend, which has proven to be a useful tool for the task, is the use of *analytical seismic fragility curves*. Generally, these curves show the probability of a structure sustaining certain levels of damage when it experiences a seismic event at a given intensity level. Figure 2 illustrates how a fragility curve is interpreted. Four stages of structural damage are typically used: slight, moderate, extensive and complete. The seismic intensity is usually represented by Peak Ground Acceleration (PGA) and the probability of damage is shown as a percentage on the y-axis.

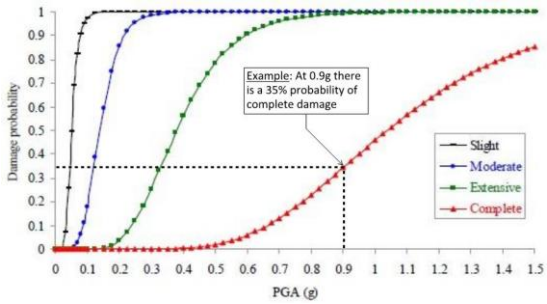

Figure 2: Explanation of how to read a fragility curve (Zirakian and Boyajian, 2016)

By using fragility curves for a seismic event, one can systematically determine affected routes and their recovery time, leading to more efficient emergency response plans. Figure 3 shows how fragility curves can be assigned to various bridges in a network. Immediately after an earthquake, network managers will know which bridges could still function (depending on the earthquake intensity) and hence communicate to the public which routes are safer to use.

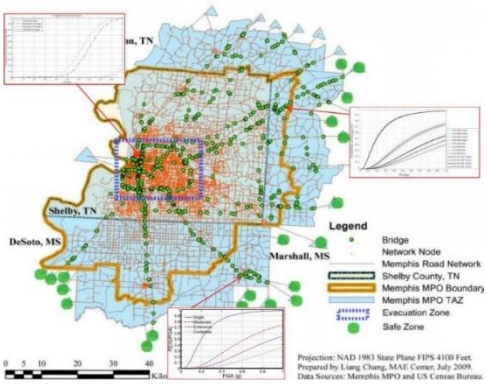

Figure 3: Fragility curves used in the management of a transportation network (Chang et. al, 2012)

But how does one know if the given fragility curve is a true representation of the structure? It depends on how accurate one models the bridge behaviour during an earthquake, as well as using realistic enactments of the ground motions.

One of the biggest assumptions made in the structural analysis of bridges is related to the foundation and in-situ properties. Indeed, numerical models for this have either simplified the real foundation behaviour or used some empirical formulations to cater for uncertainties associated with the in-situ characteristics.

Hence, a more accurate modelling of the Soil-Structure Interaction (SSI) would improve the accuracy of the fragility curves abovementioned, for instance. Moreover, the SSI should be better analysed and understand how this can lead to an

improvement in the accuracy of the fragility curves and ultimately, lead to a better decision on asset management.

This report aims to assess how different models on the simulation of soil-structure interaction can better predict the performance of a bridge under seismic loading. In complement, the cost in using such techniques (with respect to time and effort) will be assessed towards a better understanding on how they might be useful from the perspective of bridge assessment and design.

Three main aspects of the overall topic will be looked at in this report:

- How would different SSI analysis models influence the accuracy of representing the bridge behaviour during an earthquake?
- What would be the difference in analyses results if the foundation model was based upon the type of site profile where the bridge is located instead of varying the soil parameters?
- What effect will the different SSI modelling have on fragility curves?

Three common types of SSI models: Winkler springs, Lumped springs and dashpots (substructure approach), and Direct method using finite elements to represent the soil.

Hence, the following four objectives are outlined for the scope of this work:

- Determine the difference in probabilities of bridge failure depending on two different site conditions. Specifically, liquefaction would occur in one of the two sites.
- Compare the resulting fragility curves when three different types of SSI analysis are used.
- Relate their differences in failure-probabilities to the analysis run-times required. Reference can also be made to complex software requirements for any analyses.
- Compare the differences in bridge deck displacements for the three types of SSI analysis (in terms of selecting appropriate bearings).

Further to this introductory section, a literature review about fragility curves and previous case studies on the topic are presented first. Then, various models of a reference bridge are created and analysed to observe the differences in results and fragility curves. Finally, the most relevant conclusions are drawn at the end of this report as well as further steps that are envisaged by the author.

II. LITERATURE REVIEW

2.1 HOW ARE FRAGILITY CURVES DERIVED?

"*A fragility function or curve is a probabilistic tool used to estimate the damage likely to occur during a seismic event. It is given explicitly as the probability of meeting or exceeding some limit state for a specific intensity of seismic excitation*." (Nielson, 2005)

Figure 4 shows two different curves derived for the same structure and using the same seismic ground motions. On the left, it is showed a 25 % probability of failure, for a certain scenario and at 0.4g, whereas on the right, a probability of 85 % is showed for almost the same scenario.

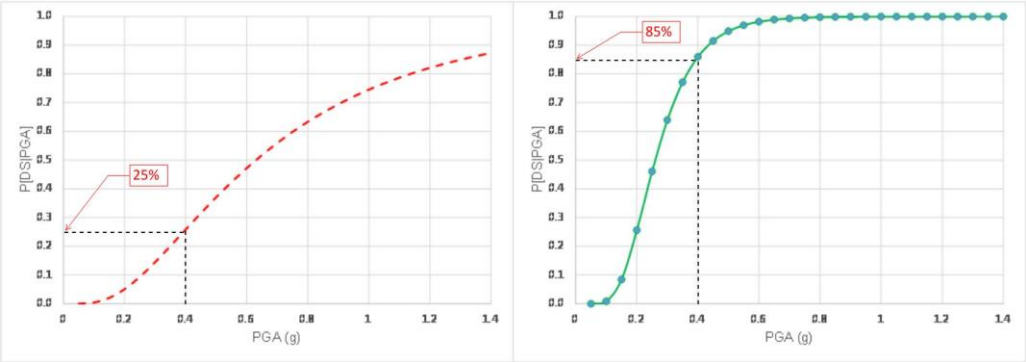

Figure 4: Fragility curves by (Nielson, 2005) left and (Bowers, 2007) right

Hence: Which curve would, or should, the network operators rely on to make the best decision on the maintenance of the structure above? In order to answer this, it is important that these curves become, as much as possible, reliable so that they can be used with the required degree of confidence. Indeed, the difference between both cases, in terms of values of probabilities, is a consequence on the assumptions taken into account beforehand (i.e. in the level and quality of the bottom line information).

Based on the assumption that seismic demands and bridge capacities follow lognormal distributions (Cornell et al, 2002), the fragility-curve is expressed by means of Eq. (1).

$$P[D>C|\mathrm{IM}] = \Phi\left[\frac{\ln(S_d/S_c)}{\sqrt{\beta_{D|IM}^2+\beta_c^2}}\right] \quad (1)$$

Where:

$\Phi[\,]$ is the standard normal distribution function

S_d is the median estimated seismic demand

S_c is the median estimated structural capacity

$\beta_{D|IM}$ is the dispersion of the seismic demand based on intensity measure

β_c is the dispersion of capacity.

2.1.1 Probabilistic Seismic Demand Models (PSDM)

The seismic demand, S_d, is usually better estimated by means of a Probabilistic Seismic Demand Model (Cornell et al, 2000) which can take the general form as shown by Eq. (2).

$$\ln(S_d) = \ln(a) + b\ln(IM) \tag{2}$$

This is related with the demand to a chosen Intensity Measure (*IM*), which is generally preferred to be Peak Ground Acceleration (*PGA*) according to Neilson (2006), who also showed that PSDMs can be derived using the following procedure:

1. Compile a suite of ground motion records appropriate for the region under investigation;
2. Create an adequate number of statistical samples (i.e. analytical models of the bridge structure). The models would be different by their material strengths, soil parameters, etc;
3. Perform a seismic analysis for each pair of ground-motion and bridge model by recording the outputs of interest with correspondence to the peak values from the *IM*;
4. Conduct a regression analyses to derive the PSDM and $\beta_{D|IM}$.

It should be noted that the PSDM described above is in relation to the bridge components. By using a crude Monte Carlo simulation, they can be used to form a Joint Probabilistic Seismic Demand Model (JPSDM) to determine bridge system fragility.

2.1.2 Capacity Of Structure: Limit States For The Bridge Components

Determining bridge capacities in terms of limit states require two main factors: (i) selection on the components to be monitored and (ii) quantifying the threshold values beyond which the components are considered to fail under loading.

The calculation of these two factors goes far beyond the scope of this report nevertheless, a full description on suitable methods can be found elsewhere (Nielson, 2005). Some of the bridge components presented and monitored by Nielson (2005) are also adopted in this report.

Under the scope of the subject under analysis, four qualitative limit states are typically defined, mainly: Slight, Moderate, Extensive and Complete damage. These are combined with quantitative values, by means of Bayesian updating, to obtain the median and dispersions limit states related to the component.

2.1.3 Fragility Curves And SSI Modelling

The seismic demand is mainly affected by the chosen suite of ground motions, and the type of models used for analyses. Hence, the probabilities of reaching the above limit states due to a specific seismic demand will be different, depending on the type of SSI model used to simulate the bridge foundation.

2.2 TYPICAL MODELS USED FOR SSI

2.2.1 Non-Linear Winkler Springs (P-Y Curve Approach)

This method is widely used for pile foundations because of its simplicity and minimal computational effort required. In this case, the soil is modelled by means of non-linear springs representing varying stiffness of a layered soil profile.

Figure 5 illustrates an example related to the lateral, axial and end-bearing foundation interactions and how this is modelled with springs. More specifically, the lateral springs are defined by non-linear soil resistance-displacement relationships or, as well known, by p-y curves. According to Lombardi & Bhattacharya (2016), these p-y curves are set based on procedures recommended by the *American Petroleum Institute* (API) and *Det Norske Veritas* (DNV).

Dash and Bhattacharya (2017) proposed a method for improving these p-y curves by taking into account the soil behaviour in liquefiable soils. It is worth to mention that this method is considered in this report.

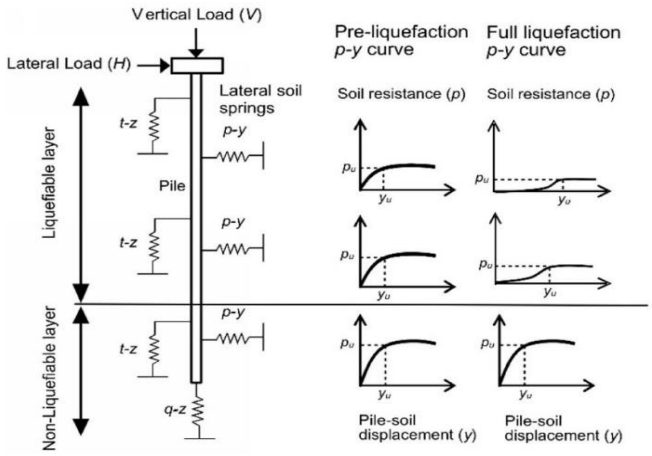

Figure 5: Non-Linear Winkler spring model (Dash and Bhattacharya, 2017)

2.2.2 Lumped Springs & Dashpots (Substructure Method)

This method is more elaborated and it may require a significant amount of initial analyses to set-up the final SSI model to be employed on the seismic analysis of the bridge. Nevertheless, once this is done, i.e. the calculation of the foundation constants, the time required for the seismic analysis is relatively small and with minimal computational effort.

Schematically, Figure 6 illustrates how the structure and soil are modelled – i.e. as separate models or substructures. On the soil side, the foundation reactions to loading are converted to spring constants K_{xx}, $K_{\phi\phi}$, $K_{x\phi}$ or impedance functions, which are then used in the structural model.

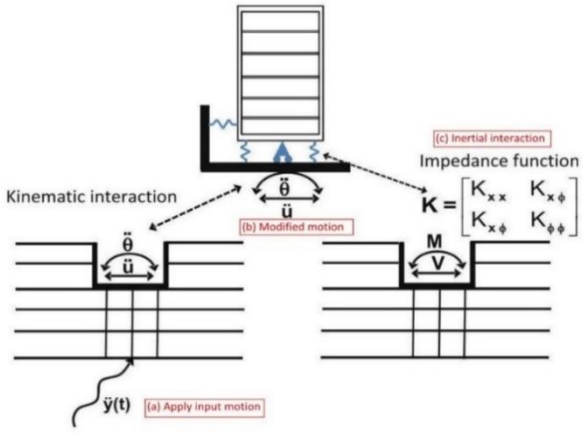

Figure 6: Substructure method (Pecker, 2007)

Several formulas are available in the literature that allow to calculate these foundation constants (ASCE 4-98, EN 1998-5, Gazetas, 2006) even though most of them are limited to one homogeneous layer or certain foundation shapes. This might reveal to

be very limited in real applications where accurate results are aimed (as the case here under analysis). Hence, and in order to take into account multi-layered soil profiles, the software *ALP* is be used to generate the foundation stiffness values for analysis of the superstructure.

2.2.3 Direct Method Using Finite Elements To Model Soil

Finally, and perhaps the most complex and robust method available is by using the Finite Element method, which usually requires higher levels of computational effort and time consuming; This option is mainly preferred when 3D analysis is required. This method is usually employed only in cases where the bridge has a significant socio-economic impact, i.e. sensitive projects that may lead to serious cases of litigation if significant damage takes place.

Similar to what was done for the previous cases, Figure 7 illustrates how the soil and structure are modelled, in this case together and as one system. The layered soil profile is defined as a continuum divided into triangular, linear strain elements. In contrast to the previous two methods, soil properties are defined by alternative parameters such as Poisson ratio, modulus of elasticity, etc. The bridge structure is modelled as beam, plate and other structural elements.

The refinement degree of the mesh and location of the boundaries will affect the accuracy of the results, as well as the required computational time. In this report, the software *PLAXIS* is used to perform this analysis.

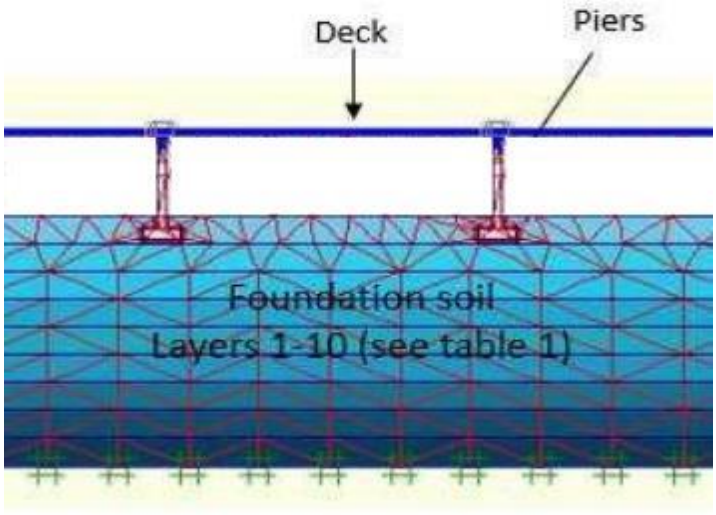

Figure 7: Structure and soil modelled together using finite elements

2.3 CASE STUDIES AVAILABLE IN THE LITERATURE

Five cases are presented mainly related to: (i) the use of bridge classes to produce generalised fragility curves, (ii) comparison of SSI effects on fragility curves (iii) liquefaction effects, (iv) the effect of probability assumptions on the overall analyses and (v) SSI effect on bridge components.

2.3.1 Work Done By Nielson (2005) And Bowers (2007)

Nielson (2005) analysed and categorised the bridge classes by acknowledging the high costs involved to produce individual fragility curves for bridges in a network, so that each curve will represent a range or family of bridges. The most meaningful results are showed in Table 1 which lists the eleven classes of bridges determined. The last column in Table 1 shows the percentage of each class from the overall population and it gives an idea about which bridge classes are most common.

Table 1: Bridge classes determined for Central and South-eastern United States (Nielson, 2005)

Name	Abbreviation	Number	Percentage
Multi-Span Continuous Concrete Girder	MSC Concrete	10,638	6.5%
Multi-Span Continuous Steel Girder	MSC Steel	21,625	13.2%
Multi-Span Continuous Slab	MSC Slab	5,955	3.6%
Multi-Span Continuous Concrete Box Girder	MSC Concrete-Box	916	0.6%
Multi-Span Simply Supported Concrete Girder	MSSS Concrete	30,923	18.9%
Multi-Span Simply Supported Steel Girder	MSSS Steel	18,477	11.3%
Multi-Span Simply Supported Slab	MSSS Slab	9,981	6.1%
Multi-Span Simply Supported Concrete Box Girder	MSSS Concrete-Box	4,909	3.0%
Single-Span Concrete Girder	SS Concrete	22,793	13.9%
Single-Span Steel Girder	SS Steel	18,281	11.2%
Other		18,945	11.7%
Total		163,433	100%

Moreover, the author produced analytical fragility curves for ten of the bridge classes in Table 1. It is worth to mention that the above bridge classes have been widely accepted and used by numerous other research, some of which are included below.
With further reference to Table 1, Bowers (2007) researched the Multi-Span Simply Supported Concrete Girder (MSSS Concrete) class, but with consideration for liquefaction, which was not taken into account before. His bridge configuration was exactly the same as the one presented by Nielson (2005) as shown in Figure 8.

For this, a Winkler-spring model was used for analyses in the software *OpenSees*, and the p-y springs were factored to model liquefaction behaviour as shown in Figure 9.

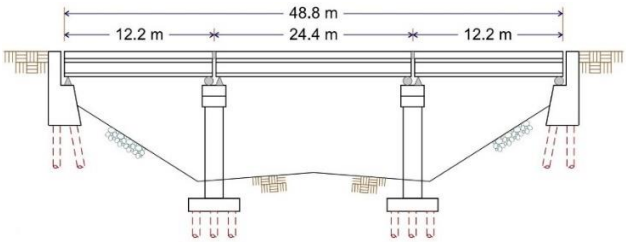

Figure 8: Configuration of the reference bridge used by (Nielson, 2005) and (Bowers, 2007)

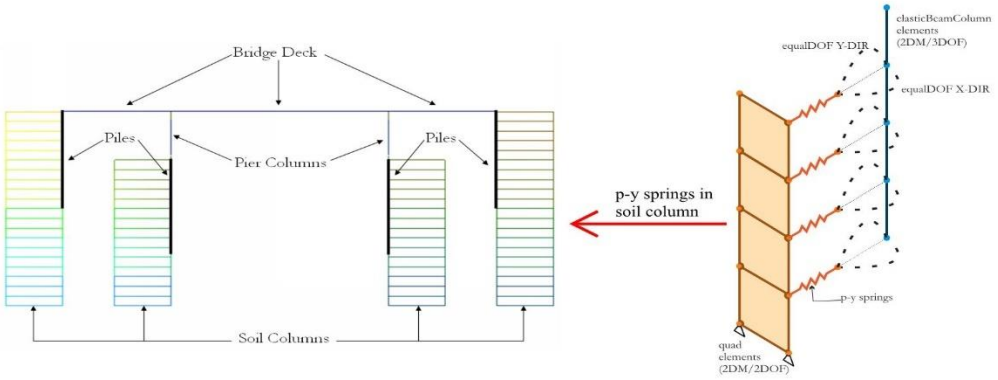

Figure 9: Winkler spring model in OpenSees software used by Bowers (2007)

In Figure 10, the results obtained for the fragility curves are presented and compared for the same bridge, using similar ground motions and without considering liquefaction. Bowers (2007) obtained higher levels of failure probabilities because of the SSI modelling method, which has been used to derive the PSDMs.

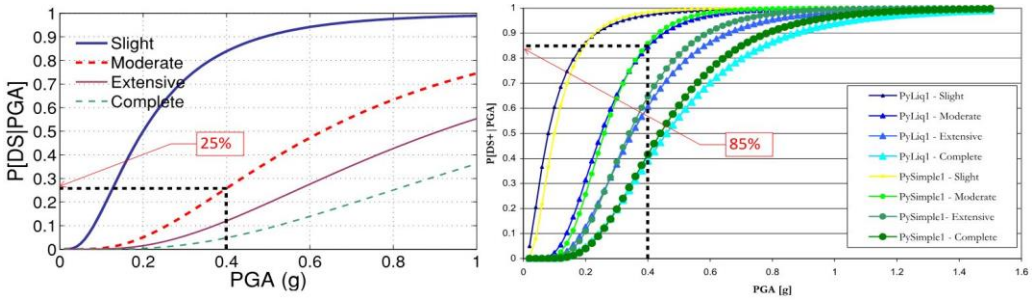

Figure 10: Fragility curves by (Nielson, 2005) left and (Bowers, 2007) right

2.3.2 Work Done By Kwon And Elnashai (2010)

Kwon & Elnashai (2010) analysed the behaviour of another class of the bridges listed in Table 1 – Multi-Span Continuous (MSC) Steel Girder.

As shown in Figure 11, the bridge model comprises four spans - 2 @ 14m and 2 @ 18m. The deck is supported on circular piers, which are connected to pile caps founded on 10 steel piles. Each of the abutments is anchored by 6 steel piles.

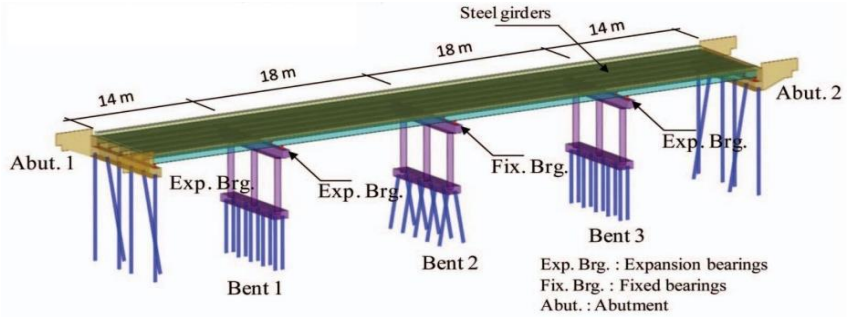

Figure 11: Configuration of the reference bridge used

The authors used four methods for modelling the bridge foundations, mainly: (i) fixed-base, (ii) lumped springs derived using conventional approaches (e.g. analysis results from the software *LPile*), (iii) lumped springs derived using FEM analyses and (iv) 3D finite element models of the soil and pile foundation. The site condition for the bridge was assumed to be mostly stiff to hard clay soil layers. Despite the approach made, there was no evidence which method led to more accurate fragility curve. The reason for this was related to insufficient and reliable data.

Instead, Kwon & Elnashai (2010) opted to rely on the curve derived by using the multi-platform/3D finite element approach since this method was described and verified experimentally in a previous paper (Kwon et. al, 2008). Figure 12 shows the compared results of the study where the 'Multiplatform' curve was determined to be more reliable.

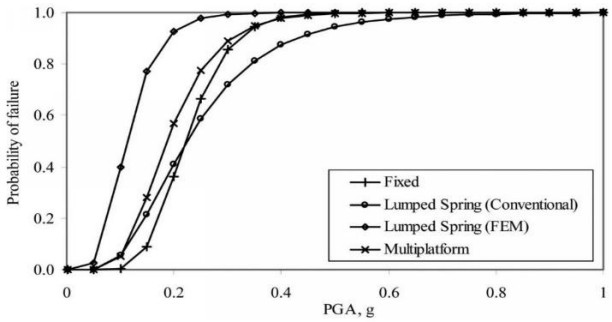

Figure 12: Fragility curves obtained using the four methods (Kwon & Elnashai, 2010)

2.3.3 Work Done By Zong (2015) And Aygun Et. Al (2010)

In this case, the authors focussed on MSC steel girder bridge, as classified by (Nielson, 2005), even though Zong (2015) has considered a bridge with a slightly longer span.

Similar to the work done by Bowers (2007), Aygun et. al (2010) considered liquefaction effects, and used the software *OpenSees* to create a 3D bridge model linked to 2D

soil elements by p-y springs. These analyses were only made for the longitudinal direction of the bridge. Based on their method of analysis, the authors concluded that liquefaction increases the probability failures for most bridge components, which is in agreement with what was expected.

Zong (2015) used two types of foundation models for comparison, mainly: (i) fixed-base and (ii) Winkler springs. Both analyses were done in 3D using the software *OpenSees*. The author concluded that the probability of failure for both the bridge system and the individual components, decreased when SSI effects are included.

It is worth to mention that although both authors studied the same bridge class, the utilization of different ground motions to derive the PSDMs led to fragility curves that cannot be compared directly.

2.3.4 Work Done By Karamlou & Bocchini (2015)

Karamlou & Bocchini (2015) analysed the same MSSS Steel Girder bridge as classified by (Nielson, 2005). Figure 13 shows how the bridge was modelled by using the lumped-spring approach, but in this case the research focused on the probability assumptions made in deriving the PSDMs.

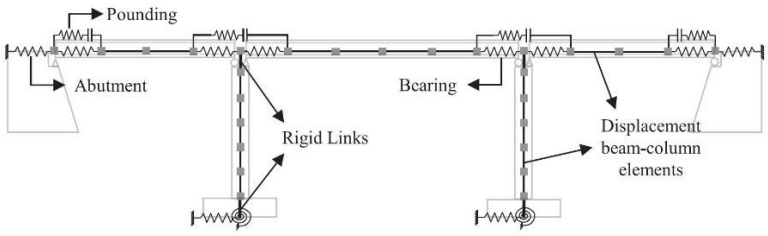

Figure 13: Configuration of the reference bridge used

The obtained results were considerably different to the ones obtained by the traditional methods. Indeed, the expected life-cycle loss in some cases were found to be up to 50% overestimated when typical probability assumptions such as *power model* and *constant dispersion* are made.

2.3.5 Work Done By Stefanidou Et. Al (2017)

Stefanidou et. Al (2017) analysed the behaviour of a 3-span (2 @ 27m, and 1 @ 45m) overpass bridge in Greece. In comparison to the previous cases presented, this is classified as a MSC Concrete Box Girder as seen in Figure 14.

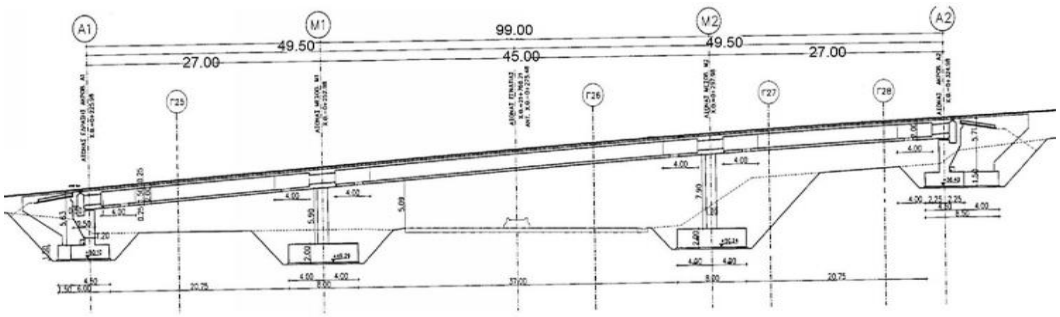

Figure 14: Configuration of the reference bridge

Similarly to Kwon and Elnashai (2010), three foundation models were compared: (i) fixed-base, (ii) lumped linear springs and (iii) translational & rotational springs and dashpots derived using the *Substructure method*. The site condition for this bridge was assumed to be Site Class B - stiff soil (Eurocode 8, Part 1, 2004). Furthermore, this bridge used shallow foundations as opposed to pile foundations in the other cases.

On the contrary to the conclusions drawn by Zong (2015), the authors found that the abutments (at component level) had a higher failure probability when a detailed SSI analysis is considered. Although this difference could be due to the fact that the authors modelled a shallow foundation as stated before. Nevertheless, bridge component fragility is an important factor for retrofit designs, and they should be more accurately predicted.

Kwon and Elnashai (2010) also found detailed SSI analysis resulted in a lower probability of the system failure, when compared to the case of fixed-base and/or other model types. Figure 15 illustrates how the detailed SSI curves, shown in red colour, are the lowest of the three methods in all four limit states: LS1, LS2, LS3 and LS4.

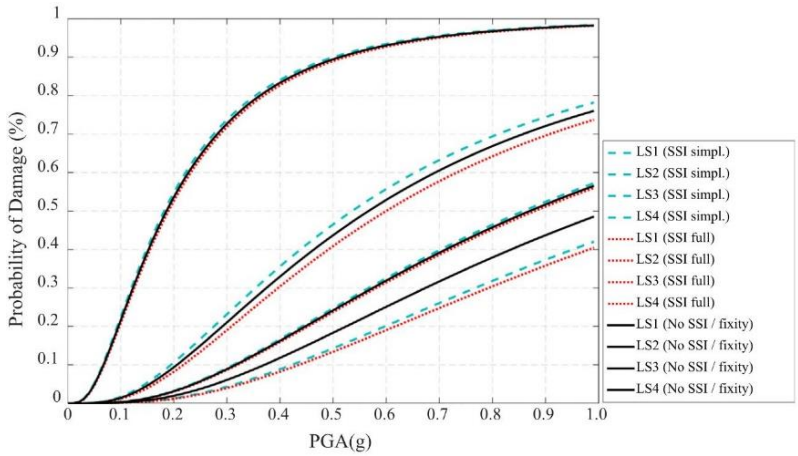

Figure 15: Fragility curves in longitudinal direction comparing SSI methods (Stefanidou et. al, 2017)

2.4 COSTS OF ANALYSIS (IN THE CONTEXT OF TIME & EFFORT)

Zong (2015) noted that the 3D time-history analysis for each case in his research took more than 2 days computational time per case. Karamlou & Bocchini (2015) had a relatively large number of analyses to conduct based on their chosen statistical method. They took approximately 15 hours to perform all required analyses. Computational time taken for the analyses in this report will be recorded and compared to the subsequent results in Chapter 5.

2.5 GAPS OBSERVED IN STATE-OF-THE-ART METHODS

Further to the presented cases, the following gaps have been identified:

- Variances in soil parameters were used to treat different site profiles as opposed to comparing two sites at different ends of a site classification spectrum,
- Only one type of SSI analysis model was used to examine the effects of liquefaction, as opposed to the three types proposed in this report,
- The research with different SSI methods is inconsistent; with one having inconclusive results, and the other two having conflicting results.
- Where layered soil profiles were used, its effect on the seismic input motions are unclear or not even explained,
- No information is available on the costs associated with the different levels of modelling.

Therefore, the objectives of the work in Chapter 3 can be outlined as follows:

- Determine the difference in probabilities of bridge failure when two different soil profiles/sites are considered for the same bridge;
- Compare the resulting fragility curves when three types of SSI analyses are used: (i) Winkler springs (ii) Substructure (iii) Finite element;
- Estimate the costs associated with the different levels of analyses and relate the costs to the differences in analyses results;
- Compare the differences in bridge deck displacements for the three types of SSI analyses (in terms of selecting appropriate bearings).

III. CASE STUDY, METHODS & FE MODELLING

3.1 INTRODUCTION

With respect to the gaps observed in the literature review, this chapter explains the methodology for achieving the objectives listed in the previous section 2.5. An overview of the sections in this chapter is best understood by a flowchart as shown in Figure 16, which links each section to the sequence of work required for achieving the desired objectives.

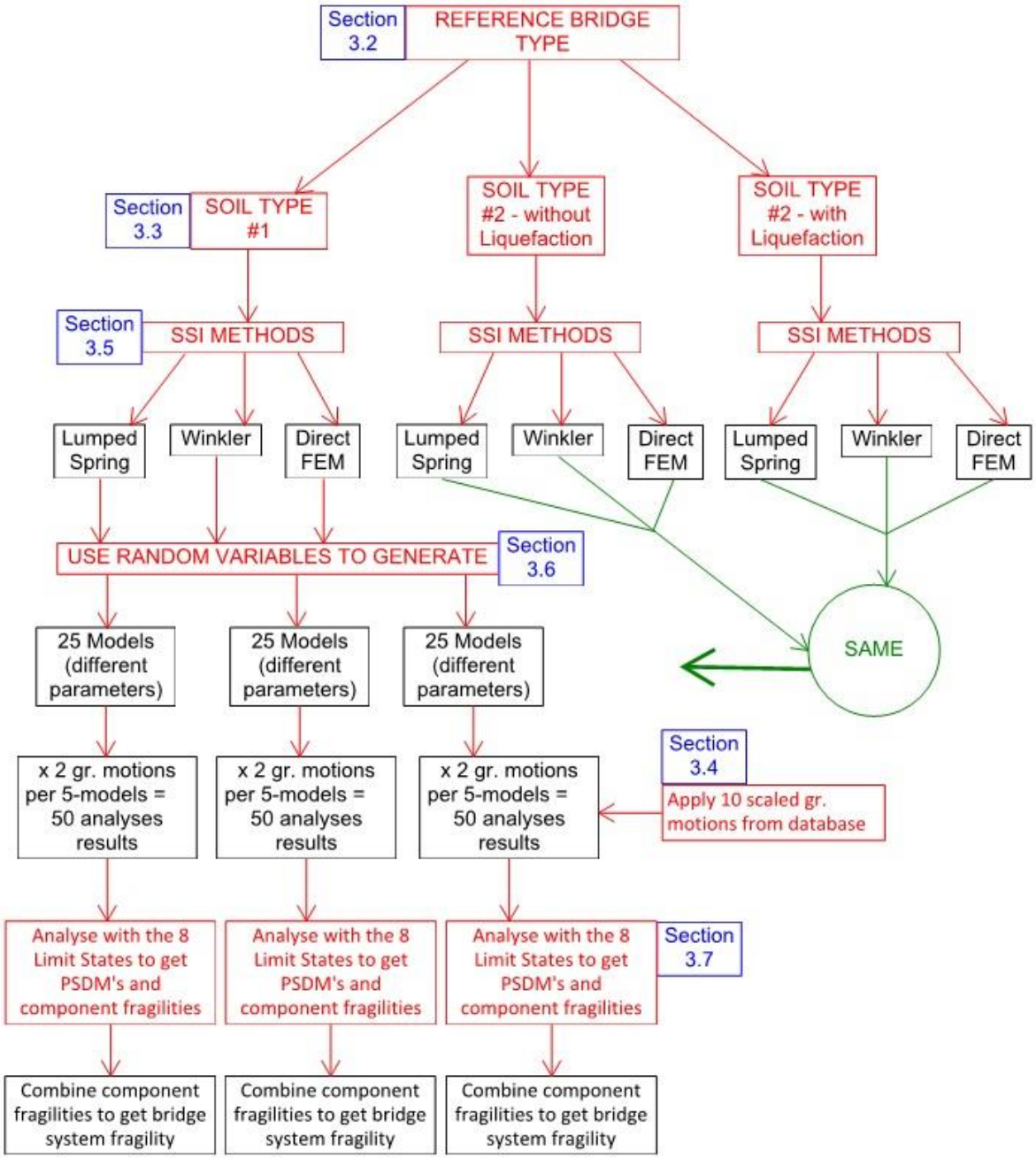

Figure 16: Flowchart outlining the work sequence of Chapter 3

3.2 CASE STUDY: THE BRIDGE TYPE

The bridge type selected for the scope of this work is a MSC Steel Girder type, which has been chosen on the basis to draw relationships from some of the case studies previously introduced in the Literature review (Chapter 2). Indeed, this is a typical bridge which represents approximately 13 % of the Central and South-eastern United States total bridge population (Nielson, 2005).

The geometry of the selected MSC Steel Girder bridge is illustrated in Figure 17. The superstructure entails 3 equal spans of 30.3 m. The deck width is 15 m and comprises a 0.178 m thick slab on 8 no. steel plate type girders. Rocker bearings connect the deck to the abutments, whereas fixed bearings are used above the intermediate piers.

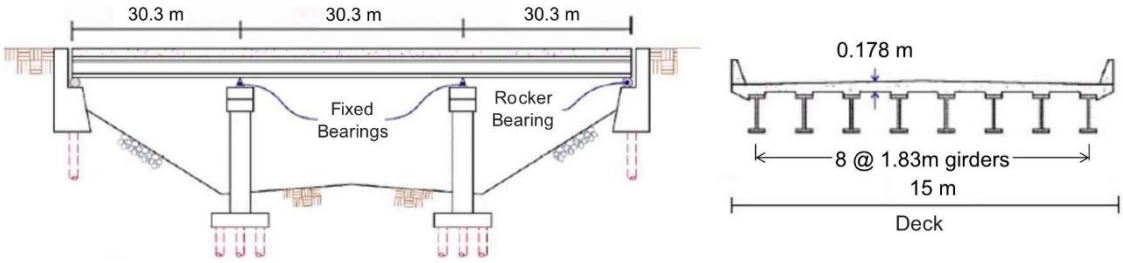

a) Bridge elevation *b) Typical cross-section*

Figure 17: MSC Steel Girder bridge

The abutments have a back-wall height of 2.4 m and sits on a 4 m wide strip footing anchored to the ground by 10 piles. Figure 18 shows the configuration of each pier support, with 3 circular columns @ 4.5 m high and 0.9 m Ø. A 1 m wide × 1.2m deep capping beam sits on top of the piers. The pier pile-group foundation is shown in Figure 19 which consists of a 3 m square × 1 m thick pile cap on 8 no. square piles.

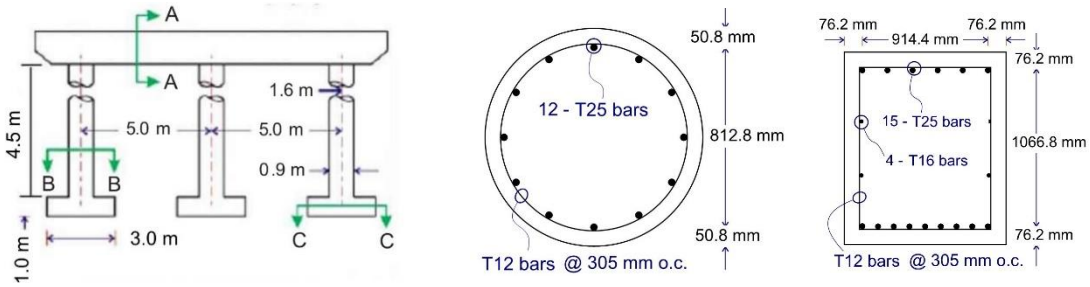

a) Pier elevation *b) Section B-B* *c) Section A-A*

Figure 18: Pier configuration and details

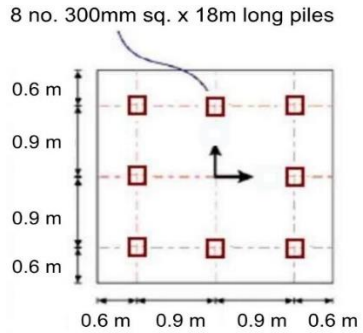

Figure 19: Pile cap and pile-group details

3.3 CASE STUDY: THE TYPE OF SOILS

Further to the objectives outlined for this project (Chapter 1), two soil profiles are considered, where one of them correspond to a site with potential to liquefy. In order to achieve real-world scenarios, actual borehole data are used from two sites: BBFL Consultants (2016) and Bhattacharya et al. (2014).

Regarding the potential of the soil liquefying, Eurocode 8 is used to perform the analysis on both sites, mainly by:

- Using BS-EN 1998-1:2004, the 'Ground Types' and 'Soil Types' are determined based on the N_{SPT} values at each level;
- Unit weights, γ, of the soil layers are assumed based on correlations to N_{SPT} values (ENGM054 Earthquake Engineering, 2018);
- The Seismic Shear Stress and Cyclic Stress Ratio (CSR) can be calculated and used with the SPT to check against charts in BS-EN 1998-5:2004 to determine whether the soil layer will liquefy.

The tabulated calculation values are shown together with the sketches of each soil profile below. It is worthwhile to mention that these are typical soil profiles for this type of bridges.

The first soil profile (Figure 20) is related to a site predominantly with clay and silt layers with high N_{SPT} values and therefore, it does not have the potential to liquefy. This profile has been extracted from a bridge site in Sangre Grande, Trinidad (BBFL Consultants, 2016).

On the other hand, a second soil profile (Figure 21) is related to a site where layers are sand and the top 16 m has the potential to liquefy. This is profile has been extracted from the Showa Bridge site (Bhattacharya et al, 2014).

Even though the soil profile #2 could liquefy at certain magnitude earthquakes, non-liquefiable p-y curves are still constructed in the next Section in order to make better comparisons between the sites.

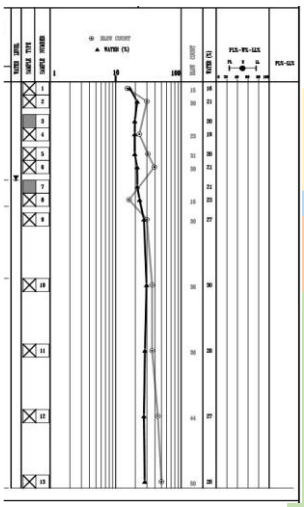

	Depth, z (m)	N_{SPT}	γ (kN/m^3)	Seismic Shear Stress τ_e (kN/m^2)	σ_{vo}' (kN/m^2)	Cyclic Stress Ratio	Result
Stiff Sandy Clayey Silt	0.4	15	16	0.96	2.40	0.40	No Liquefaction
	1	30	19	2.84	9.00	0.32	No Liquefaction
	2.5	23	17	6.35	17.50	0.36	No Liquefaction
	3.5	31	19	9.94	31.50	0.32	No Liquefaction
Stiff Sandy Silt	4	39	19	11.36	36.00	0.32	No Liquefaction
	5.5	16	17	13.98	38.50	0.36	No Liquefaction
Hard Sandy Clayey Silt	6.5	30	19	18.46	58.50	0.32	No Liquefaction
	9.5	36	19	26.98	85.50	0.32	No Liquefaction
	12.5	36	19	35.51	112.50	0.32	No Liquefaction
	15.5	44	19	44.03	139.50	0.32	No Liquefaction
Hard Silty Clay	18.9	50	19	53.69	170.10	0.32	No Liquefaction
							continue last value up to 30m depth

Figure 20: Details of Soil Profile #1

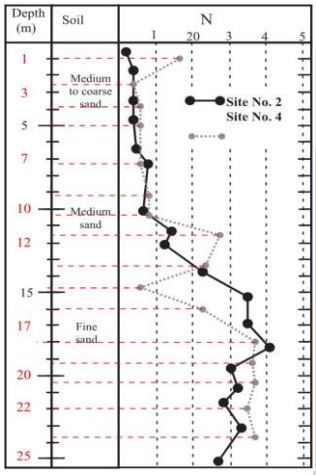

	Depth, z (m)	N_{SPT}	γ (kN/m^3)	Seismic Shear Stress τ_e (kN/m^2)	σ_{vo}' (kN/m^2)	Cyclic Stress Ratio	Result
Medium to coarse sand	1	17	18	2.69	8.00	0.34	Liquefaction
	2.5	4	16	5.98	15.00	0.40	Liquefaction
	3.8	6	16	9.09	22.80	0.40	Liquefaction
	5	6	16	11.96	30.00	0.40	Liquefaction
Medium sand	7.25	6	16	17.34	43.50	0.40	Liquefaction
	9.25	8	16	22.13	55.50	0.40	Liquefaction
	10.4	8	16	24.88	62.40	0.40	Liquefaction
	11.5	27	18	30.95	92.00	0.34	Liquefaction
	13.3	23	18	35.79	106.40	0.34	Liquefaction
	14.7	6	16	35.16	88.20	0.40	Liquefaction
Fine sand	16	23	18	43.06	128.00	0.34	Liquefaction
	18	37	19	51.13	162.00	0.32	No Liquefaction
	19.25	36	19	54.68	173.25	0.32	No Liquefaction
	20.3	37	19	57.66	182.70	0.32	No Liquefaction
	22	35	18	59.20	176.00	0.34	No Liquefaction
	23.7	37	19	67.32	213.30	0.32	No Liquefaction
							continue last value up to 30m depth

Figure 21: Details of Soil Profile #2

3.4 CASE STUDY: GROUND MOTION DATABASE

Among several possibilities, the ground motion selected for this work is extracted from the 1964 Niigata earthquake (Kudo and Kanno, 2000). Indeed, this ground motion was recorded for the case of soil profile #2, in Japan (Bhattacharya et al, 2014). The

record was obtained from the Earthquake Research Institute website of the University of Tokyo (University of Tokyo, 2018). The data was scaled to create 10 independent record datasets, ranging, in PGA from 0.1, 0.2, 0.25, 0.3, 0.35, and 0.4 to 0.8 g (supported by MATLAB, 2017). As an illustrative example, Figure 22 shows one of the 10 independent record datasets (see *Appendix A* for the remaining).

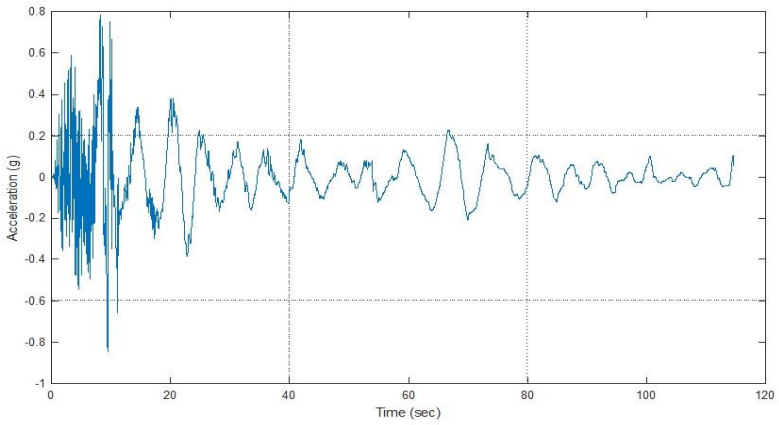

Figure 22: Scaled ground motion acceleration record from the 1964 Niigata earthquake

It is worth to mention that the scaled motions are applied directly to the soil base layer for the case of the direct FE modelling approach, which is located much deeper, when compared to the pile foundation depth (i.e. 18 m) that is used for the the Winkler and Lumped-Spring models. Hence, modified ground motions are obtained at the pile level (which are derived from the direct FE modelling approach) and these are the motions which are applied to the Winkler and Lumped-spring models.

Finally, it is also important to note that the 10 sets of ground motion are combined with the 25 bridge models to perform all the analyses needed to define the PSDM. Hence, a combination of 2 sets of ground motion to every 5 bridge models gives a total of 50 analyses under the scope of this work.

3.5 METHODS: SOIL-STRUCTURE MODELLING

3.5.1 Winkler Springs Using Api & Liquefaction P-Y Curves

The Winkler springs are represented by non-linear p-y curves derived from the method stated in the American Petroleum Institute (API) 21st Edition (American Petroleum Institute, 2000). The software *ALP* (Analysis of Laterally-loaded Piles) from Oasys (2017) is used to automatically generate the coefficients required to setup the respective p-y curves.

- **Soil profile #1: non-liquefiable soil**

Due to the fact that the foundations of the bridge have groups of piles (Figure 17 and Figure 18), the group effect is necessary to be accommodated by using the p-multipliers, as recommended by Brown & Reese (1988). Basically, this method involves scaling the p-values by a factor which is a ratio of the soil resistances, between an average group pile, and a single pile. An example of the tabulated results is shown in Table 2, which shows the p-multiplier in the last column, and the corresponding p-y curve is shown in Figure 23.

Table 2: Calculation of p-y curve taking into account the pile-group effect (soil profile #1).

Node	γ_{soil} [kN/m³]	$P_u = p_{ui}$ [kN/m]	A	k [kN/m³]	H [m]	$p_{ug} = \frac{1}{n} p_{ui}$	$p_{mult} = p_{ug}/p_{usp}$
1	16.00	**72.78**	0.9	17,777	0.50	**9.10**	**0.559**
2	6.00	**150.23**	0.9	17,777	2.00	**18.78**	**0.287**
3	6.00	**409.95**	0.9	17,777	4.00	**51.24**	**0.213**
4	6.17	**1,003.10**	0.9	23,676	6.00	**125.39**	**0.211**
5	6.42	**1,951.10**	0.9	23,676	8.67	**243.89**	**0.272**
6	6.56	**3,195.60**	0.9	23,676	11.33	**399.45**	**0.334**
7	6.64	**4,736.50**	0.9	23,676	14.00	**592.06**	**0.396**
8	6.81	**9,396.40**	0.9	42,427	16.00	**1,174.55**	**0.346**
9	7.06	**12,132.00**	0.9	42,427	18.00	**1,516.50**	**0.384**

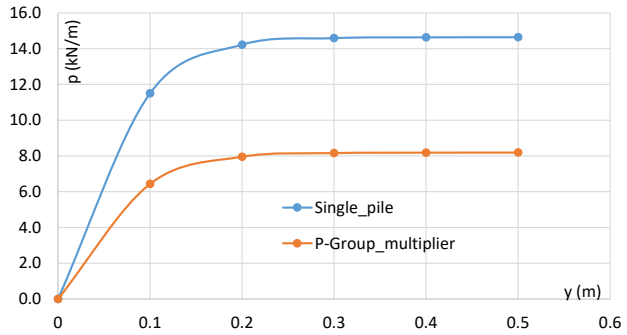

Figure 23: P-y curves with and without group effects (soil profile #1).

- **Soil profile #2: liquefiable soil**

For the specific case of liquefiable soils, the p-y curves were constructed by using the method proposed by Dash and Bhattacharya (2017), as mentioned in Chapter 2. Similar to the previous case, the same p-multipliers, to take into account the pile group effect, are also applied to the case of liquefaction curves. Taking into account the complexity for this case, an example of the full calculation used to construct the curve can be found in *Appendix B* and a sample of the resulting p-y curve for liquefied soil is shown in Figure 24.

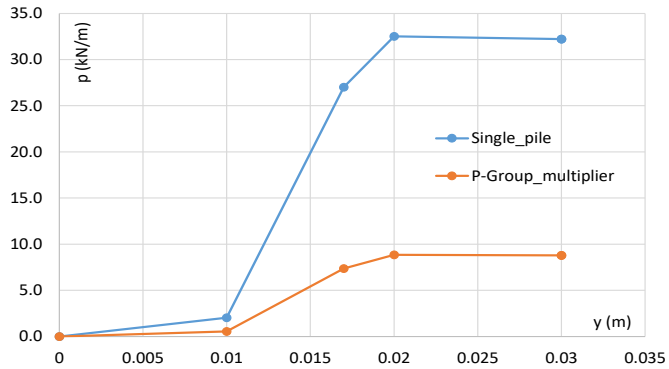

Figure 24: P-y curves with and without group effects (soil profile #2-Liquefied).

3.5.2 Lumped Springs: Deriving Pier and Abutment Springs

Taking advantage that under the scope of this work a full pile foundation is also considered, it can be further used to determine the lumped spring parameters. A single pile cap with its 8-piles is analysed separately to derive p-y curves for use as the pier foundation lumped-springs. This is done by applying increasing horizontal loads to the pile-cap and record corresponding displacements to plot a p-y curve. Similarly, increasing moments are applied to the model and corresponding rotations are plotted to obtain a lumped-rotational spring constant in kNm/rad.

For the vertical springs, the skin friction per pile-section is calculated by the standard geotechnical formulas: $k_o \sigma_v \tan \delta$ or S_u multiplied by the pile surface area (depending on whether the soil is sand or clay respectively). Similar to before, increasing vertical loads are applied to determine a lumped-vertical spring constant.

For sake of simplicity and efficiency, a model of the abutment is analysed using the FE software package, in a very similar manner to the pier foundation presented before. The only difference is that for the abutment model, the embankment-backfill stiffness is taken according to Caltrans (Nielson, 2005).

For illustration, Figure 25 shows two of the load-displacement curves obtained from the analysis models. It should be noted that for the abutment springs only, the same spring parameters are used in both the Winkler and lumped-spring models.

3.5.3 Direct Finite Element Method

The main difference between this method and the previous two is related to the fact that the soil is now modelled with suitable finite elements instead of springs.

This approach requires additional parameters to be defined for the soil profiles. Correlation tables, which use empirical formulas to suggest relationships between different soil parameters, are used to obtain the additional parameters (ENGM054 Earthquake Engineering, 2018). Under the scope of this project, Table 3 summarizes the values of interest for both soil profiles (i.e. #1 and #2), where the known soil parameters of γ_{avg}, S_u and Φ are matched with values of shear modulus and Poisson's ratio obtained from the correlation tables.

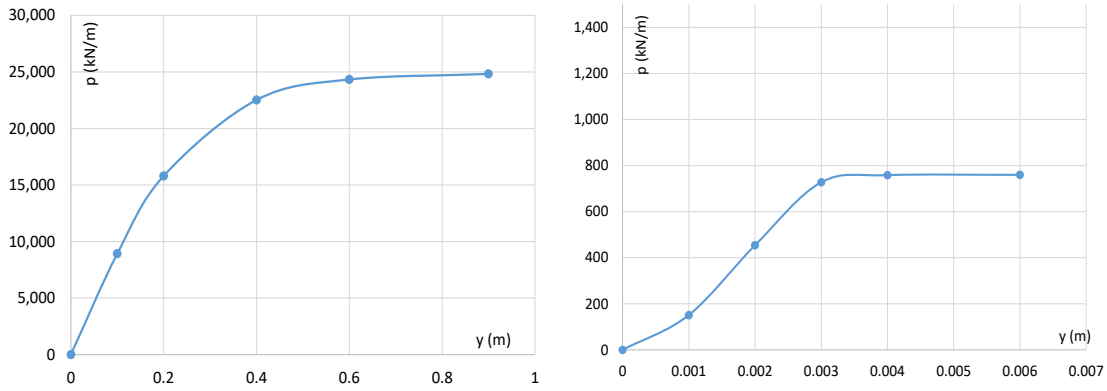

(a) Soil Profile #1 *(b) Soil Profile #2 - Liquefied*

Figure 25: P-y curves for the longitudinal abutment spring parameter

Table 3: Soil parameters obtained from correlations to SPT values (ENGM054 Earthquake Engineering, 2018)

	SOIL PROFILE #1 - CLAY				SOIL PROFILE #2 - SAND			
	S_u (kN/m^2)	γ_{avg} (kN/m^3)	Shear modulus, G (kN/m^2)	Poisson's ratio, v	Friction angle, Φ (°)	γ_{avg} (kN/m^3)	Shear modulus, G (kN/m^2)	Poisson's ratio, v
Layer 1	155	17.0	60,000	0.40	32	16.0	20,000	0.35
Layer 2	235	19.0	65,000	0.40	35	17.0	55,000	0.30
Layer 3	155	18.0	60,000	0.40	40	19.0	230,000	0.25
Layer 4	248	19.0	100,000	0.35	N/A	N/A	N/A	N/A

3.6 METHODS: RANDOM VARIABLES & LIMIT STATES

3.6.1 Random Variables

Since the selected bridge type, i.e. MSC Steel Girder bridge, is a typical class/family of bridges (it represents 13 % of the total bridge population, as abovementioned), it is worthwhile to consider a scenario where only material properties and some geometric features might have some variability (i.e. from one bridge to another): Hence, these variabilities can be used to create the various bridge models that are required to perform the aimed fragility analyses. Based on the state-of-the art presented

beforehand (Karamlou and Bochini, 2015 Nielson, 2015), and under the scope of this project, five bridge properties have been identified as random variables, which are showed in Table 4.

Table 4: Random variables and their probabilistic distributions

Random variable	Distribution type	Parameter 1		Parameter 2		Units
Steel strength	Lognormal	λ =	6.13	ξ =	0.08	Mpa
Concrete strength	Normal	μ =	33.8	σ =	4.3	Mpa
Deck mass	Uniform	*l* =	0.9	*u* =	1.1	%
Fixed Bearing coefficient of friction	Lognormal	λ =	-1.56	ξ =	0.5	
Rocker Bearing coefficient of friction	Lognormal	λ =	-3.22	ξ =	0.5	

Further to the set of random variables presented in Table 4, 25 sets, each one corresponding to a specific bridge configuration, was created by using the Latin Hypercube Sampling (LHS) method. More specifically, 5 values were quantified based on the respective CDF (i.e. equally spaced points). Then, each value of this set of 5 values from each random variable is grouped with the other values from other remaining variables according to the LHS method. Hence, 25 sets were then quantified, where each group is a unique combination of the quantified values.

3.6.2 Limit States

Further to the 25 analyses, it is possible to define Limit states which represent the outputs of interest and listed in the previous section, i.e. the parameters in the fragility curve (Eq. (1)), mainly:

- S_c - the median estimated structural capacity,
- β_c - the dispersion of capacity.

Nevertheless, and as mentioned previously (section 2.1.2), the calculation of these parameters goes beyond the scope of this report. Therefore, some of the limit states presented by Nielson (2005) are adopted and shown in Table 5, by taking into account that these are straightforwardly applicable to the case under analysis (i.e. a MSC Steel Girder bridge). In more detail, each column in Table 5 represents a category of damage that ranges from 'Slight' to 'Complete'. The 'N/A' values reflect the case where the calculation results found that the abutment is unlikely to achieve a category of damage due to deformations (Nielson, 2005).

Table 5: Bayesian Updated Limit States for Bridge Components from Nielson (2005)

Component	Slight		Moderate		Extensive		Complete	
	med [S_c]	disp [β_c]	med [S_c]	disp [β_c]	med [S_c]	disp [β_c]	med [S_c]	disp [β_c]
Concrete Column [μ_ϕ]	1.29	0.59	2.10	0.51	3.52	0.64	5.24	0.65
Fixed Bearing in Long. direction [fx_L] (mm)	6.0	0.25	20.0	0.25	40.0	0.47	186.6	0.65
Fixed Bearing in Transv. direction [fx_T] (mm)	6.0	0.25	20.0	0.25	40.0	0.47	186.6	0.65
Rocker Bearing in Long. direction [ex_L] (mm)	28.9	0.60	104.2	0.55	136.1	0.59	186.6	0.65
Rocker Bearing in Transv. direction [ex_T] (mm)	28.8	0.79	90.9	0.68	142.2	0.73	195.0	0.66
Abutment-Passive [ab_P] (mm)	37.0	0.46	146.0	0.46	N/A	N/A	N/A	N/A
Abutment-Active [ab_A] (mm)	9.8	0.70	37.9	0.90	77.2	0.85	N/A	N/A
Abutment-Transverse [ab_T] (mm)	9.8	0.70	37.9	0.90	77.2	0.85	N/A	N/A

3.7 METHODS: BRIDGE COMPONENT & SYSTEM FRAGILITY

In order to derive the bridge fragility, the Joint Probabilistic Seismic Demand Model (JPSDM) is used. The JPSDM and limit state models are used in a crude Monte Carlo simulation as follows:

- The correlation coefficients between the analyses responses of the eight components are determined. This means that for each of the 8 components, a correlation is made (Microsoft Excel, 2013) between their results from the 50 analyses and presented in matrix form as shown in Figure 26;
- At a chosen PGA value, N samples are taken from the demand side and capacity side each;
- Each sample from the demand side is a combination of 2 responses with their relevant correlation coefficients from the matrix;
- Their corresponding limit states would be the sample from the capacity side;
- Eq. (3) is used to track the system failure for the N samples, and the resulting values are used in the formula shown as Eq. (4) to estimate the probability of the bridge system being in the limit state for that particular PGA;

$$I_F = \begin{cases} 1 & \text{if } (x_i, x_j) \in \mathrm{F}_{ij} \\ 0 & \text{if } (x_i, x_j) \notin \mathrm{F}_{ij} \end{cases} \tag{3}$$

$$P[LS \mid IM = a] = \frac{\sum_{i=1}^{N} I_{F_i}}{N} \tag{4}$$

- The steps are repeated for a range of PGA values and linear regression is used on the scatter-plot to estimate the mean and deviation needed to construct the system fragility curve.

	$\ln(\mu_\phi)$	$\ln(fx_L)$	$\ln(fx_T)$	$\ln(ex_L)$	$\ln(ex_T)$	$\ln(ab_P)$	$\ln(ab_A)$	$\ln(ab_T)$
$\ln(\mu_\phi)$	1.000	0.933	0.718	0.946	0.722	0.899	0.591	0.761
$\ln(fx_L)$	0.933	1.000	0.671	0.969	0.676	0.864	0.613	0.738
$\ln(fx_T)$	0.718	0.671	1.000	0.703	0.999	0.706	0.219	0.469
$\ln(ex_L)$	0.946	0.969	0.703	1.000	0.705	0.910	0.653	0.717
$\ln(ex_T)$	0.722	0.676	0.999	0.705	1.000	0.711	0.224	0.474
$\ln(ab_P)$	0.899	0.864	0.706	0.910	0.711	1.000	0.573	0.639
$\ln(ab_A)$	0.591	0.613	0.219	0.653	0.224	0.573	1.000	0.761
$\ln(ab_T)$	0.761	0.738	0.469	0.717	0.474	0.639	0.761	1.000

Figure 26: Example of a correlation matrix used to determine bridge system fragility from component fragility (Nielson, 2005)

3.8 FINITE ELEMENT MODELLING

The approach used to create FE models are similar i.e. the deck and columns are plate and beam elements while the bearings are elastic spring elements with varying stiffness. However, the foundation models differ as follows:

- **Winkler Spring**

Full pile foundations are modelled as beam elements below the piers/columns. To model the non-linear Winkler springs, five points from each p-y curve (Section 3.5.1) are used to define a multi-linear point spring along the pile as shown in Figure 27. The abutments are modelled as springs (Section 3.5.2) at each end of the deck.

- **Lumped Spring**

This is very similar to the Winkler model above but without the detailed pile foundation. The abutments are also modelled in a similar manner. However, as shown in Figure 28 the lumped springs are modelled as point springs below the piers/columns. It should be noted that the same preparatory work of p-y curves and abutment stiffness are still required if this approach were to be done as an independent analysis. Therefore the time required to derive p-y curves and other spring parameters are still included with the costs associated for this method.

- **Direct FE Method**

In this approach, two aspects of the modelling are considered i.e. structure and soil. Figure 29 shows how these two are modelled together as:

Structure:

Columns & deck are modelled as beam elements while the piles are embedded-beam elements. Unlike the springs used in the previous two methods, the abutments are modelled as full plate elements against the soil.

Soil:

The boundaries of the soil continuum, in this case, extend as follows: Longitudinal direction – 1.5 times the bridge length, Transverse direction ≈ 3 times the bridge width, and a soil depth ≈ the overall mesh width. It is worth to mention that the refinement of the soil mesh will affect accuracy of the results as well as computational time.

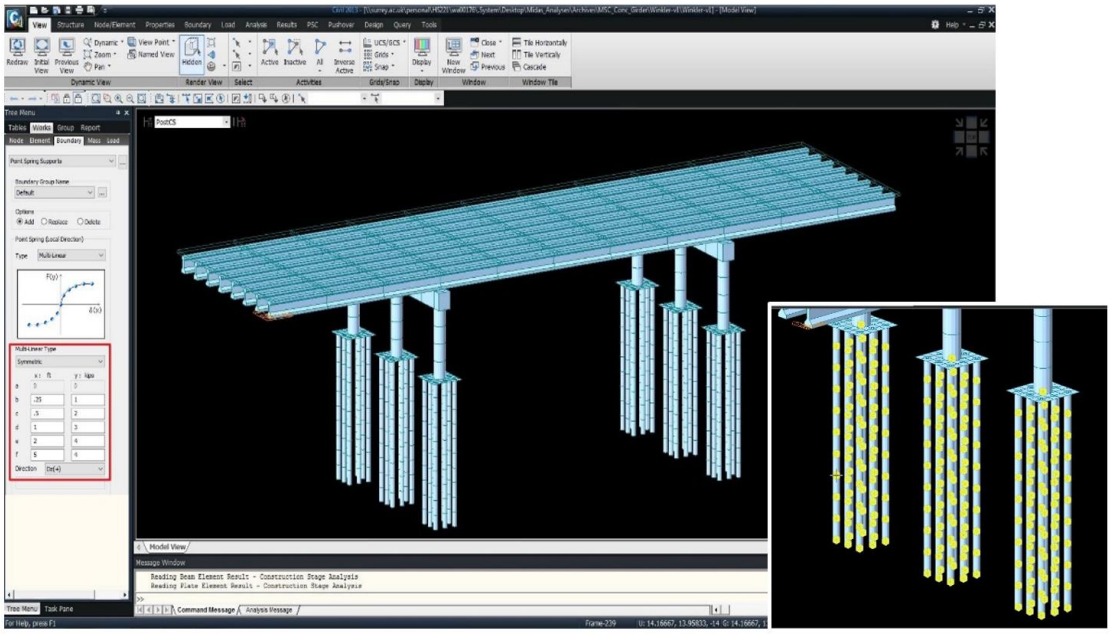

Figure 27: FE modelling with multi-linear spring (Screenshot of Midas Civil, 2013)

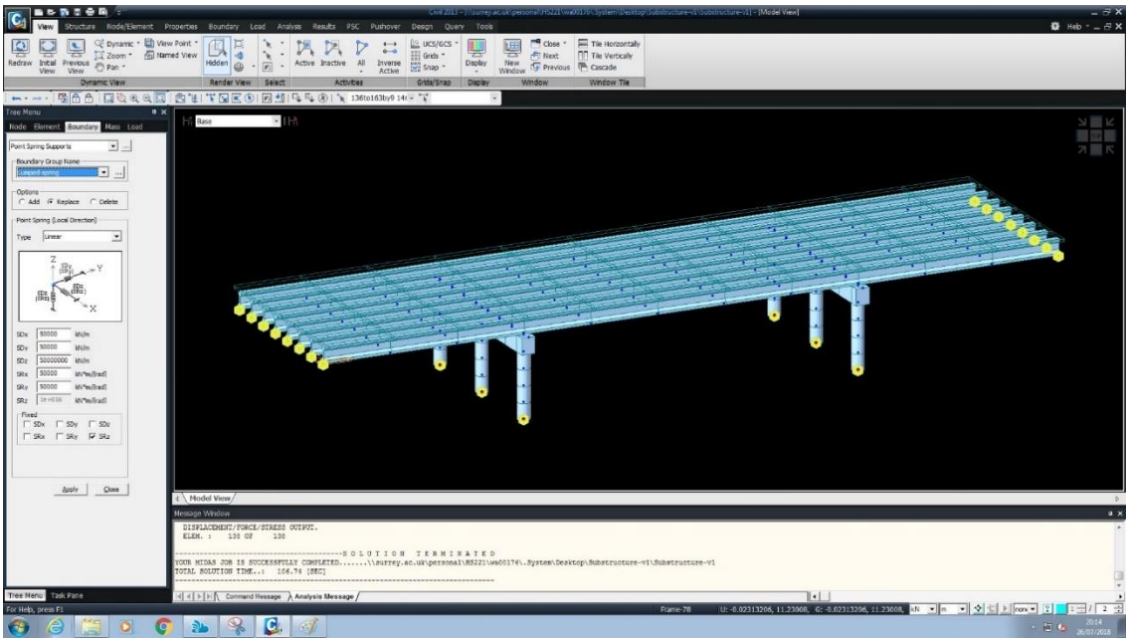

Figure 28: FE modelling with lumped-spring model (Screenshot of Midas Civil, 2013)

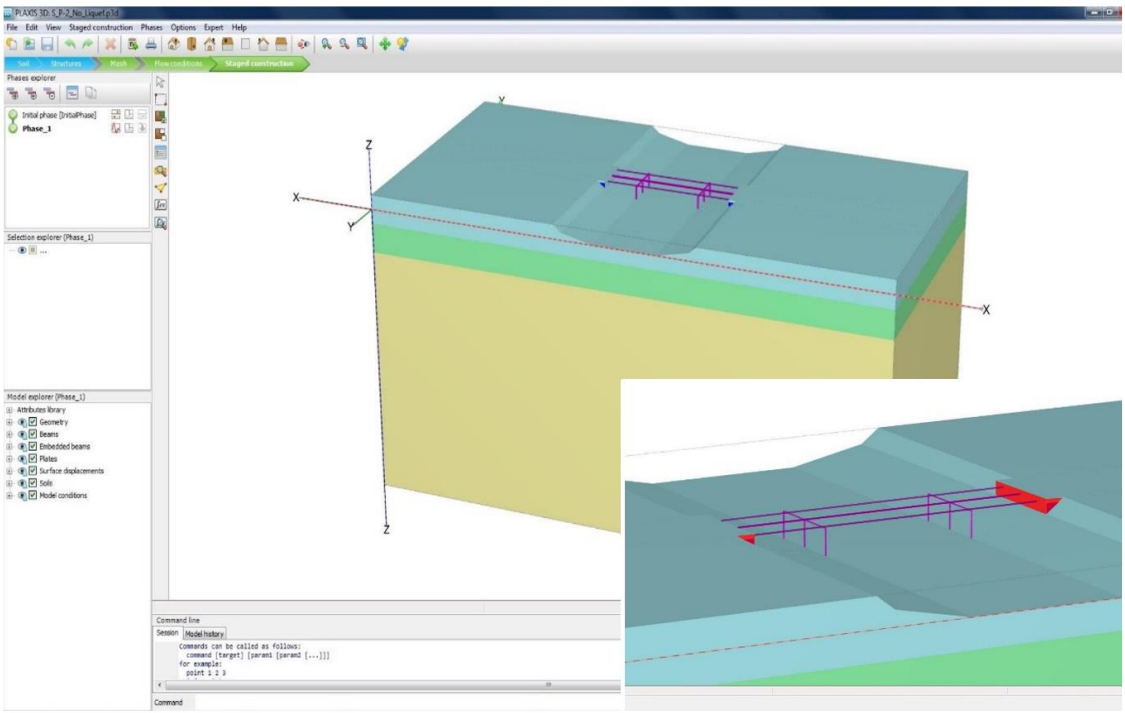

Figure 29: FE modelling with fully integration of the soil and structure (Screenshot of 3D Plaxis, 2017)

IV. RESULTS

4.1 INTRODUCTION

Further to the three approaches previously identified and outlined for simulating the soil-structure interaction, 50 analyses have been conducted by taking into account two different soil profiles (soil profile #1 and soil profile #2).

Taking into account the impossibility to present all results generated from these analyses, only the most relevant for further discussion are presented in this chapter. For further details on the complete set of results obtained, please refer to *Appendix C to E.*

In this context, a linear regression analysis has been firstly performed (Microsoft Excel, 2013) envisaging the quantification of the PSDM for each bridge component and for each soil profile. For illustration, Figure 30 shows the regression made for column curvature where the equation of the regression line relates to Eq. (2) in section 2.1.1 as:

$$\ln(S_d) = \ln(a) + b\ln(IM) \qquad (2)$$

Where: $\ln(Sd) = y$, $\ln(a) = 0.03$, $b = 1.351$ and $\ln(IM) = x$

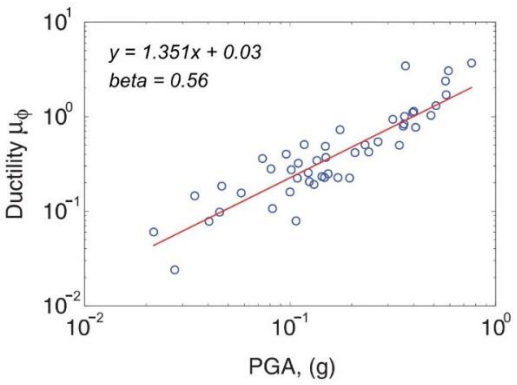

Figure 30: Linear regression for quantification of PSDM (example for the column curvature).

4.2 SEISMIC DEMAND BY THE (PSDM)

The PSDM have been quantified for the 8 bridge components, which are listed in Section 3.6.2, have been derived from analyses. In addition, taking into account that

two soil profiles have been selected for this work, one of them with potential to liquefy, allied to the fact that three approaches for the soil-structure interaction is being investigated, 9 groups of PSDM in total have been quantified. As an illustration, three of these are shown in Table 6, Table 7 and Table 8 mainly as a random case for each soil type. As it can be clearly seen, these tables are the quantification of Eq. (2), presented in Chapter 2, for the set of bridge components, aforementioned. For further details in the remaining results, please refer to *Appendix C.*

Table 6: PSDM for the bridge components (case: Winkler Spring and Soil Profile #1)

Response [ln (S_d)]	PSDM						$\beta_{D\|PGA}$
	a			*b*			
ln (μ_φ)	ln	2.34	+	0.90	*	ln (PGA)	0.37
ln (fx_L)	ln	23.79	+	1.04	*	ln (PGA)	0.56
ln (fx_T)	ln	1.52	+	1.99	*	ln (PGA)	0.52
ln (ex_L)	ln	82.27	+	1.60	*	ln (PGA)	0.75
ln (ex_T)	ln	1.69	+	3.09	*	ln (PGA)	0.97
ln (ab_P)	ln	16.97	+	1.00	*	ln (PGA)	0.49
ln (ab_A)	ln	0.60	+	0.50	*	ln (PGA)	0.59
ln (ab_T)	ln	9.09	+	0.81	*	ln (PGA)	0.44

Table 7: PSDM for the bridge components (case: Lumped Spring and Soil Profile #2 without liquefaction)

Response [ln (S_d)]	PSDM						$\beta_{D\|PGA}$
	a			*b*			
ln (μ_φ)	ln	3.10	+	1.08	*	ln (PGA)	0.45
ln (fx_L)	ln	33.68	+	1.05	*	ln (PGA)	0.61
ln (fx_T)	ln	1.64	+	2.35	*	ln (PGA)	0.57
ln (ex_L)	ln	144.46	+	1.47	*	ln (PGA)	0.66
ln (ex_T)	ln	1.87	+	3.74	*	ln (PGA)	1.09
ln (ab_P)	ln	18.16	+	1.17	*	ln (PGA)	0.53
ln (ab_A)	ln	0.67	+	0.61	*	ln (PGA)	0.67
ln (ab_T)	ln	15.30	+	1.02	*	ln (PGA)	0.54

Table 8: PSDM for the bridge components (case: Direct FE modelling and Soil Profile #2 with liquefaction)

Response [ln (S_d)]	PSDM						$\beta_{D\|PGA}$
	a			*b*			
ln (μ_φ)	ln	3.14	+	1.35	*	ln (PGA)	0.56
ln (fx_L)	ln	25.13	+	1.74	*	ln (PGA)	0.83
ln (fx_T)	ln	2.48	+	2.97	*	ln (PGA)	0.83
ln (ex_L)	ln	262.96	+	1.41	*	ln (PGA)	0.75
ln (ex_T)	ln	2.80	+	4.69	*	ln (PGA)	1.57
ln (ab_P)	ln	26.83	+	1.45	*	ln (PGA)	0.75
ln (ab_A)	ln	0.98	+	0.75	*	ln (PGA)	0.95
ln (ab_T)	ln	35.11	+	1.74	*	ln (PGA)	0.71

4.3 SOIL PROFILE #1

4.3.1 Fragility Curves For Bridge Components

To obtain a summarized version of the fragility curve data, according to the formulation in Eq. (1) (Chapter 2), this can be condensed into the form:

$$P[LS|IM] = \Phi\left(\frac{\ln(IM) - \ln(IM_m)}{\beta_{comp}}\right) \quad (5)$$

Where:

$$IM_m = \exp\left(\frac{\ln(S_c) - \ln(a)}{b}\right) \quad (6)$$

$$\beta_{comp} = \frac{\sqrt{\beta_{D|PGA}^2 + \beta_c^2}}{b} \quad (7)$$

Three example are presented in Table 9, Table 10 and Table 11 where results from 4 of the 8 components are indicated and for 2 of the 3 SSI approaches. For consistency, they represent the same cases as *Tables 6 to 8* in the previous section. The cells with values of "N/A" correspond to the 'Limit-State' values of "N/A" in Table 5 (Section 3.6.2).

Figure 31 and Figure 32 show the plotted fragility curves for some of these tables. A set of relevant tables, which have the most impact in this report, can be seen in *Appendix D.*

Table 9: Component fragility tables for (case: Winkler Spring and Soil profile#1)

Component	Slight		Moderate	
	med [IMm]	disp [βcomp]	med [IMm]	disp [βcomp]
Concrete Column [μϕ]	0.52	0.77	0.89	0.70
Fixed Bearing in Long. direction [fxL] (mm)	0.27	0.59	0.85	0.59
Rocker Bearing in Long. direction [exL] (mm)	0.52	0.60	1.16	0.58
Abutment-Transverse [abT] (mm)	1.10	1.02	5.83	1.23

Component	Extensive		Complete	
	med [IMm]	disp [βcomp]	med [IMm]	disp [βcomp]
Concrete Column [μϕ]	1.57	0.82	2.44	0.83
Fixed Bearing in Long. direction [fxL] (mm)	1.65	0.70	7.23	0.82
Rocker Bearing in Long. direction [exL] (mm)	1.37	0.60	1.67	0.62
Abutment-Transverse [abT] (mm)	14.04	1.18	N/A	N/A

Table 10: Component fragility tables for (case: Lumped Spring and Soil profile#2 without liquefaction)

Component	Slight		Moderate	
	med [IMm]	disp [βcomp]	med [IMm]	disp [βcomp]
Concrete Column [μϕ]	0.44	0.69	0.70	0.63
Fixed Bearing in Long. direction [fxL] (mm)	0.19	0.63	0.61	0.63
Rocker Bearing in Long. direction [exL] (mm)	0.34	0.61	0.80	0.58
Abutment-Transverse [abT] (mm)	0.65	0.87	2.43	1.03

Component	Extensive		Complete	
	med [IMm]	disp [βcomp]	med [IMm]	disp [βcomp]
Concrete Column [μϕ]	1.12	0.72	1.63	0.73
Fixed Bearing in Long. direction [fxL] (mm)	1.18	0.73	5.11	0.85
Rocker Bearing in Long. direction [exL] (mm)	0.96	0.60	1.19	0.63
Abutment-Transverse [abT] (mm)	4.89	0.99	N/A	N/A

Table 11: Component fragility tables for (case: Direct FE modelling and Soil Profile #2 with liquefaction)

Component	Slight		Moderate	
	med [IMm]	disp [βcomp]	med [IMm]	disp [βcomp]
Concrete Column [μϕ]	0.52	0.60	0.74	0.56
Fixed Bearing in Long. direction [fxL] (mm)	0.44	0.50	0.88	0.50
Rocker Bearing in Long. direction [exL] (mm)	0.21	0.68	0.52	0.66
Abutment-Transverse [abT] (mm)	0.48	0.57	1.04	0.66

Component	Extensive		Complete	
	med [IMm]	disp [βcomp]	med [IMm]	disp [βcomp]
Concrete Column [μϕ]	1.09	0.63	1.46	0.64
Fixed Bearing in Long. direction [fxL] (mm)	1.31	0.55	3.17	0.61
Rocker Bearing in Long. direction [exL] (mm)	0.63	0.68	0.78	0.70
Abutment-Transverse [abT] (mm)	1.57	0.64	N/A	N/A

Figure 31 and Figure 32 show the typical fragility curves obtained. A set of relevant tables, which have the most impact in this report, can be seen in *Appendix D.*

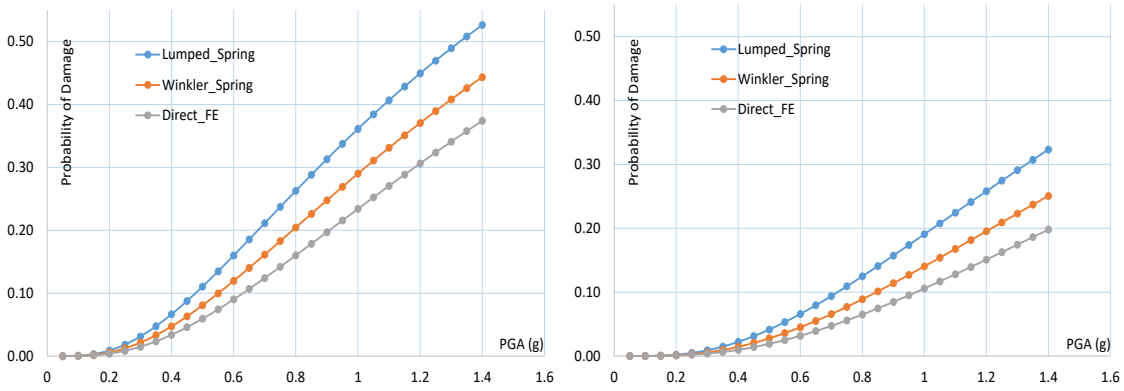

(a) Extensive damage *(b) Complete damage*

Figure 31: Concrete Column

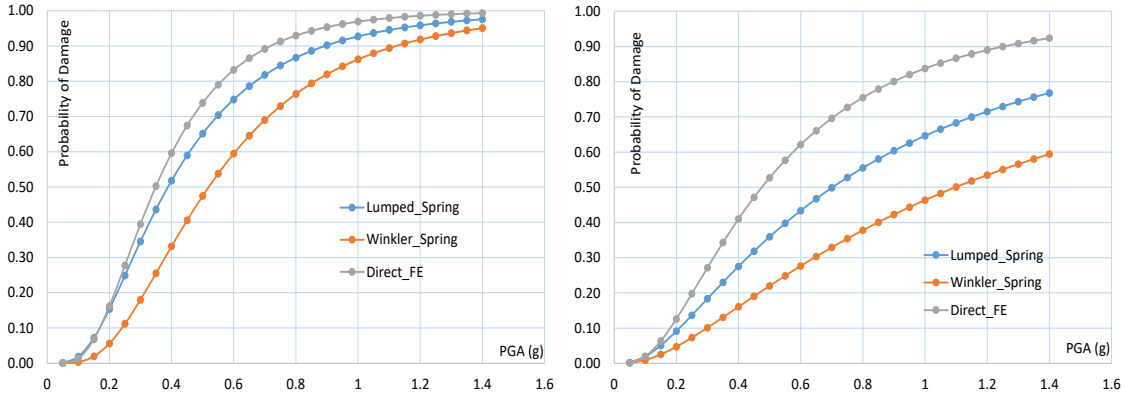

(a) Rocker bearing *(b) Abutment-transverse*

Figure 32: Rocker Bearing and Abutment-transverse (both at Slight damage)

4.3.2 Fragility Curves For The Bridge System

As mentioned in Section 3.7, the fragility curves for the bridge system is then derived from the fragility curves obtained for the bridge components by means of the correlation coefficient matrix. In relation to section 3.7, the matrix is obtained by using the "Correlation function" (Microsoft Excel, 2013) where the coefficients are determined between the ln(S_d) values obtained from the regression analysis in section 4.1. An example is shown in Table 12, which shows that the correlation between ln(fxT) and ln(ex_T) is 0.897 or the correlation coefficient between ln (abA) and ln(fx_L) is 0.639.

Table 12: Correlation coefficient matrix

	ln (μϕ)	ln (fxL)	ln (fxT)	ln (exL)	ln (exT)	ln (abP)	ln (abA)	ln (abT)
ln (μ_φ)	1.000	0.856	0.825	0.964	0.849	0.870	0.753	0.831
ln (fx_L)	0.856	1.000	0.793	0.816	0.689	0.712	0.639	0.652
ln (fx_T)	0.825	0.793	1.000	0.758	0.897	0.746	0.672	0.836
ln (ex_L)	0.964	0.816	0.758	1.000	0.861	0.855	0.753	0.791
ln (ex_T)	0.849	0.689	0.897	0.861	1.000	0.725	0.598	0.698
ln (ab_P)	0.870	0.712	0.746	0.855	0.725	1.000	0.749	0.739
ln (ab_A)	0.753	0.639	0.672	0.753	0.598	0.749	1.000	0.801
ln (ab_T)	0.831	0.652	0.836	0.791	0.698	0.739	0.801	1.000

In this context, Figure 33 shows the resulting fragility curves for the four limit states (see *Appendix E* for the System fragility tables).

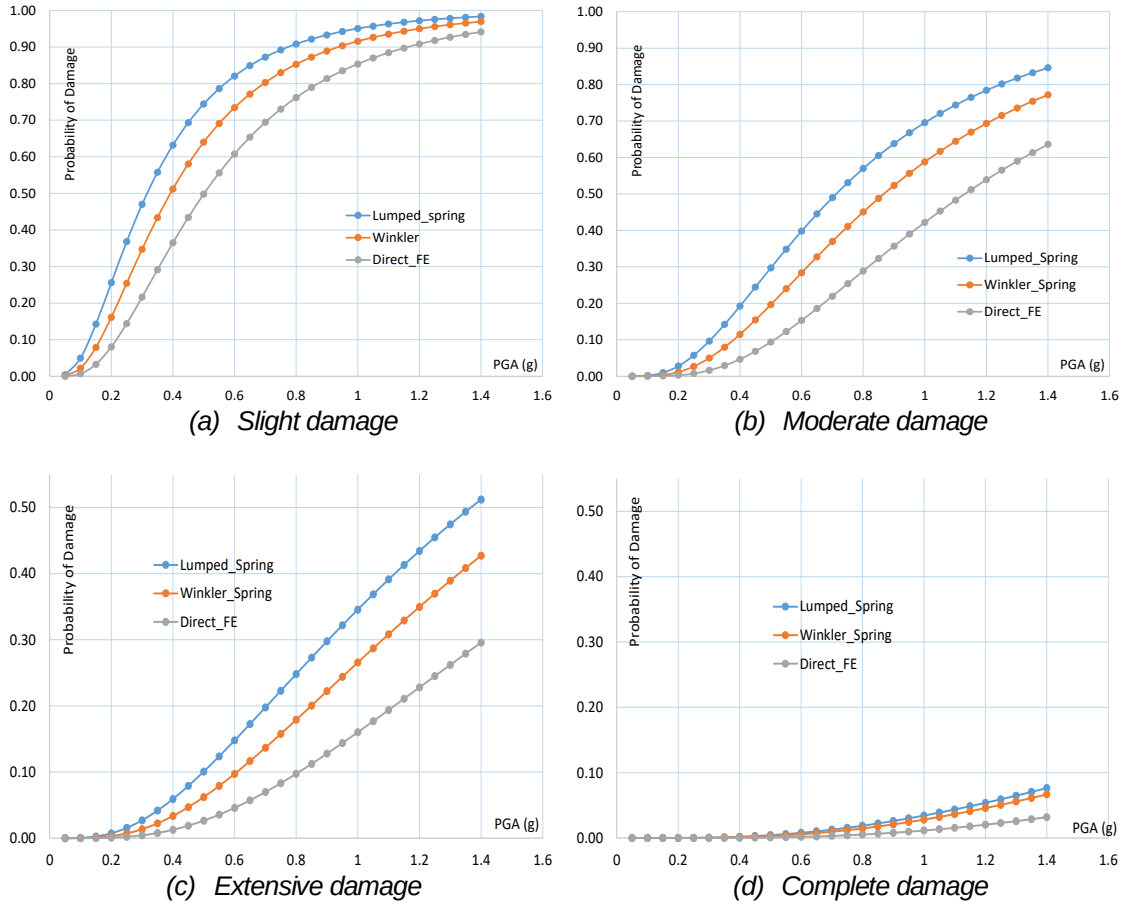

(a) Slight damage *(b) Moderate damage*

(c) Extensive damage *(d) Complete damage*

Figure 33: Bridge System fragility curves

4.3.3 ***Compare Components And Whole Bridge System***

Subsequent to the two previous sections, Figure 34 compares the results for both component and system fragility in one graph. Two cases of interest pertaining to SSI method and Damage level are presented.

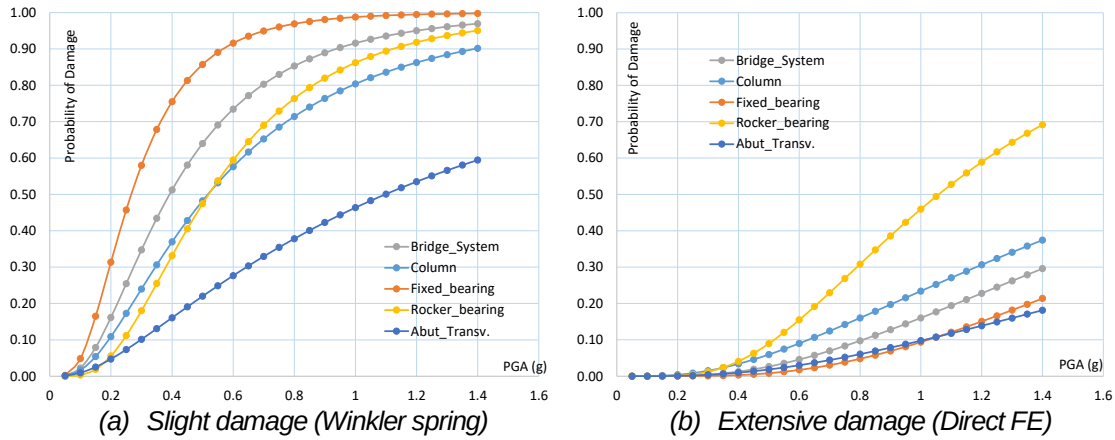

(a) Slight damage (Winkler spring) *(b) Extensive damage (Direct FE)*

Figure 34: Bridge Components vs. Bridge System

4.4 SOIL PROFILE #2 (NO LIQUEFACTION)

4.4.1 Fragility Curves For Bridge Components

Similar to the previous Section 4.3.1, Figure 35 and Figure 36 show the plotted fragility curves for some of the bridge components.

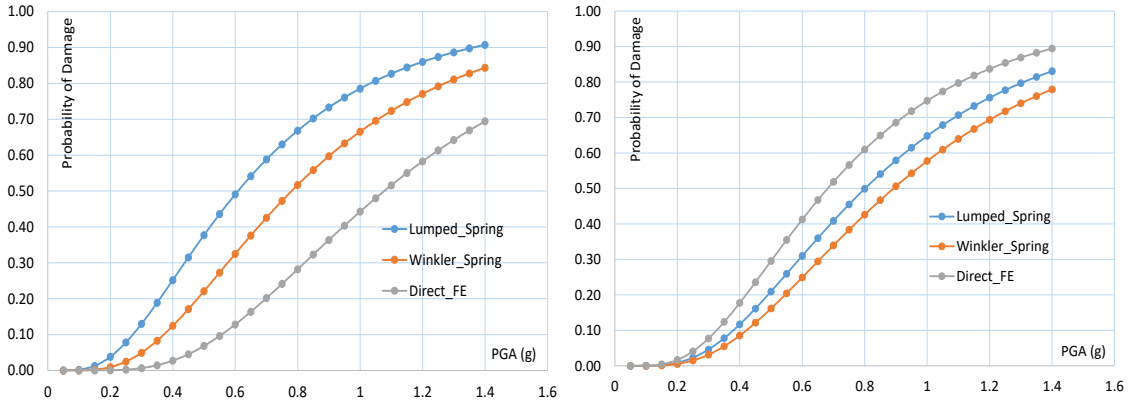

(a) Fixed bearing *(b) Rocker bearing*

Figure 35: Fixed bearing and Rocker bearing (both at Moderate damage)

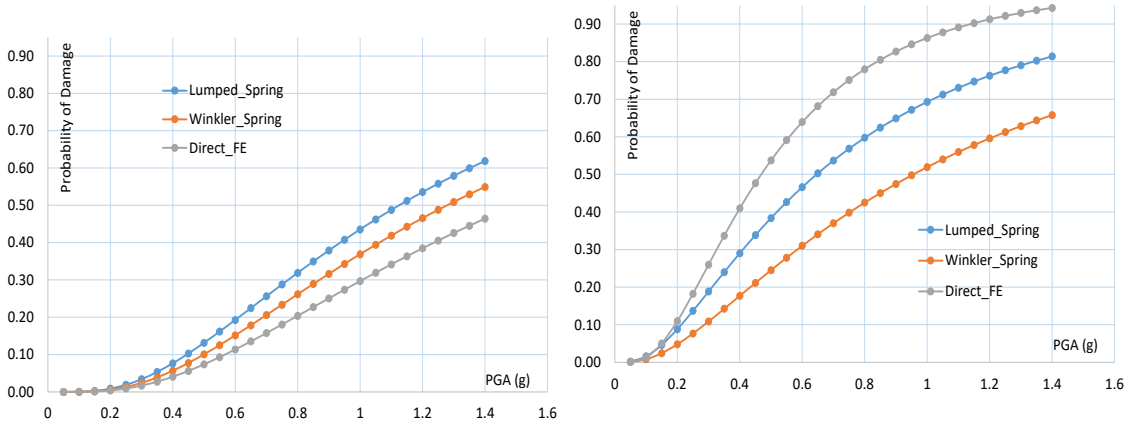

(a) Extensive damage (Column) *Slight damage (Abutment)*

Figure 36: Concrete Column and Abutment-transverse

4.4.2 Fragility Curves For The Bridge System

Again, similar to the previous Section 4.3.2, Figure 37 shows the resulting fragility curves for the four limit states

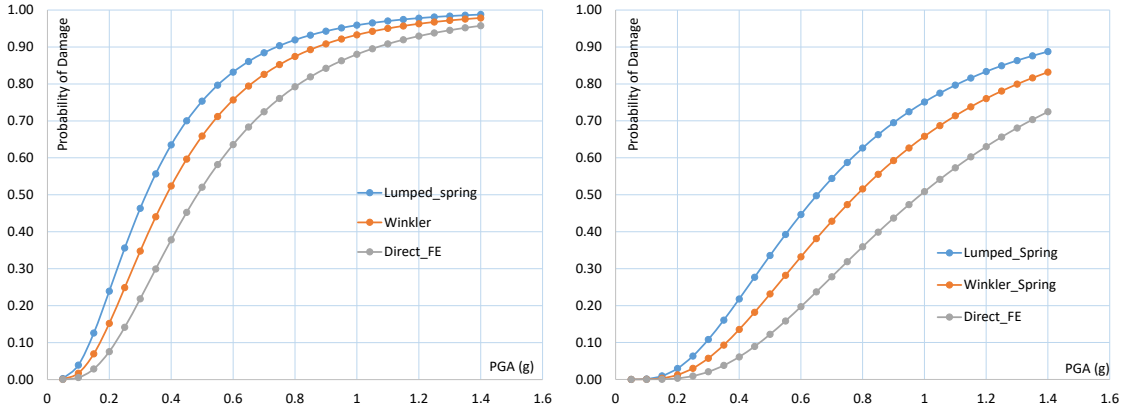

(a) Slight damage

(b) Moderate damage

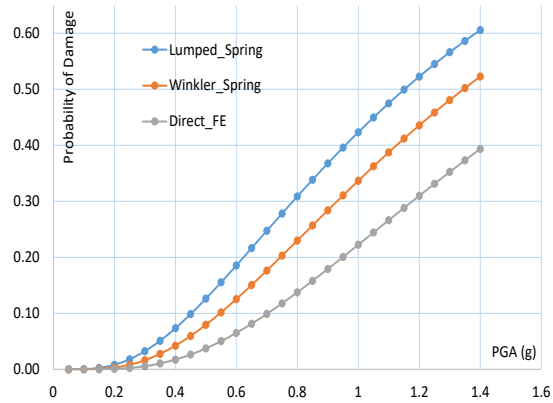

(c) Extensive damage

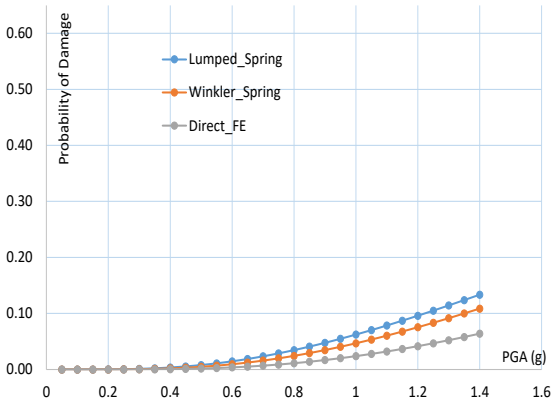

(d) Complete damage

Figure 37: Bridge System fragility curves

4.4.3 Compare Components And Whole Bridge System

Figure 38 compares the results for both component and system fragility in one graph. Two cases of interest pertaining to SSI method and Damage level are presented.

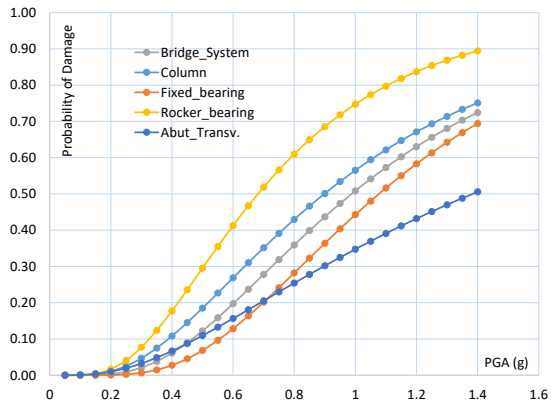

(a) Moderate damage (Direct FE)

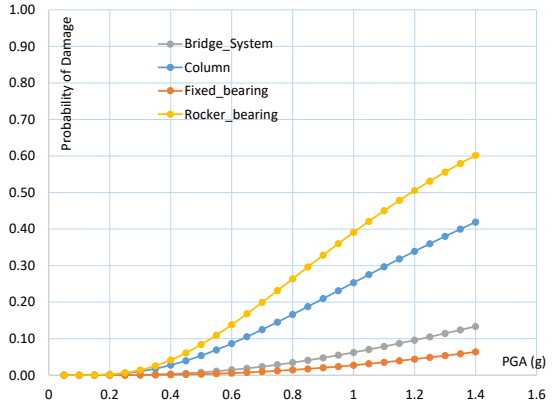

(b) Complete damage (Lumped spring)

Figure 38: Bridge Components vs. Bridge System

4.5 SOIL PROFILE #2 (LIQUEFACTION)

4.5.1 *Fragility Curves For Bridge Components*

For the last soil type considered in this report, Figure 39 and Figure 40 show the plotted fragility curves for some of the bridge components.

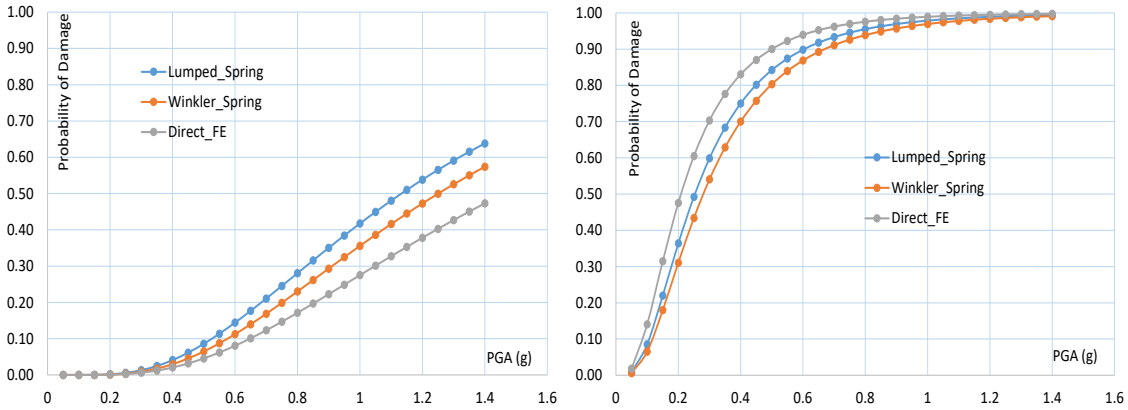

(a) Complete damage (Column) *(b) Slight damage (Rocker bearing)*

Figure 39: Concrete Column and Rocker bearing

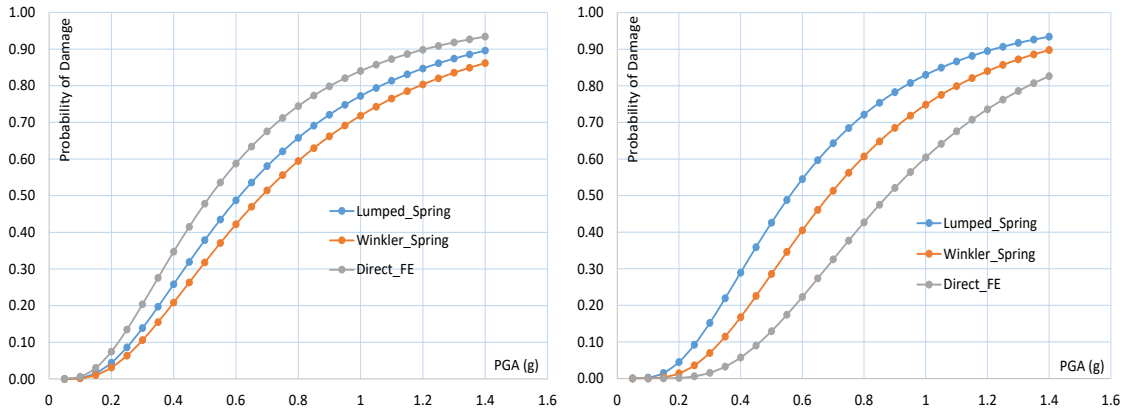

(a) Rocker bearing *(b) Fixed bearing*

Figure 40: Rocker bearing and Fixed bearing (both at Moderate damage)

4.5.2 *Fragility Curves For The Bridge System*

Figure 41 shows the resulting fragility curves for the four limit states.

4.5.3 *Compare Components And Whole Bridge System*

Figure 42 compares the results for both component and system fragility in one graph. Two cases of interest pertaining to SSI method and Damage level are presented.

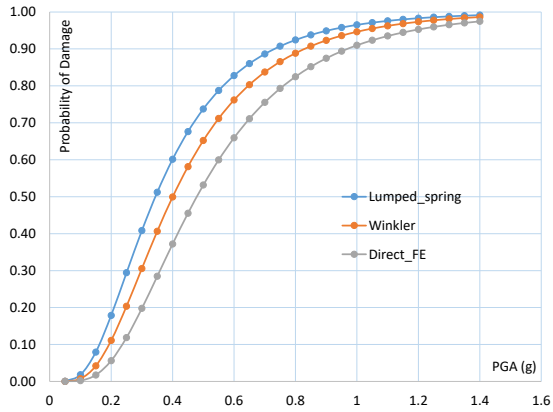

(a) Slight damage

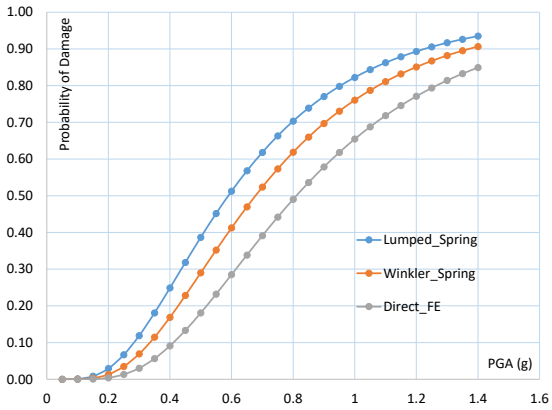

(b) Moderate damage

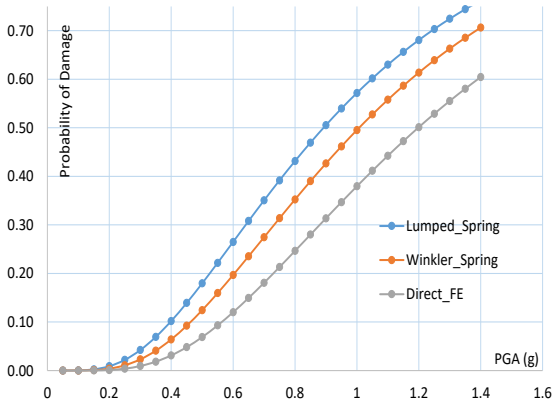

(c) Extensive damage

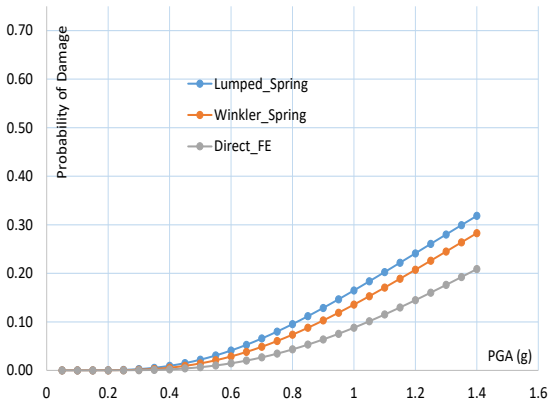

(d) Complete damage

Figure 41: Bridge System fragility curves

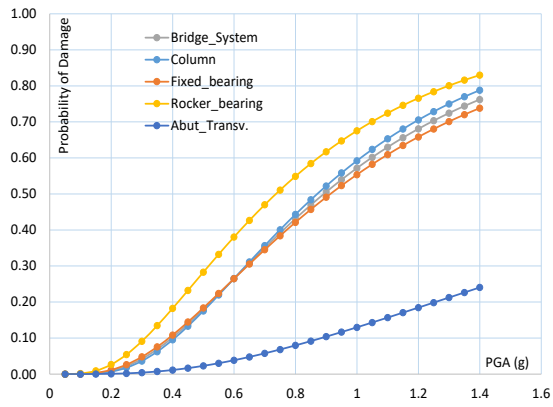

(a) Extensive damage (Lumped spring)

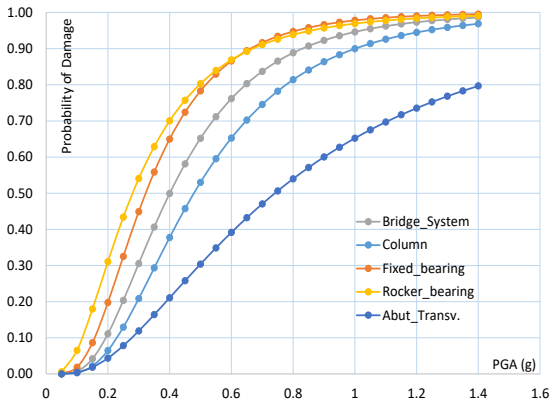

(b) Slight damage (Winkler spring)

Figure 42: Bridge Components vs. Bridge System

4.6 BRIDGE DECK DISPLACEMENTS (ROCKER BEARINGS)

The deck displacements are herein analysed due to the fact that the analyses have showed that these were indeed the higher values, overall. The same PSDMs from Section 4.1, in terms of the rocker bearing in longitudinal direction, are plotted and compared for each soil profile (Figure 43)Figure 43. However, the values are converted from logarithmic back to values that can be compared in PGA and millimetres.

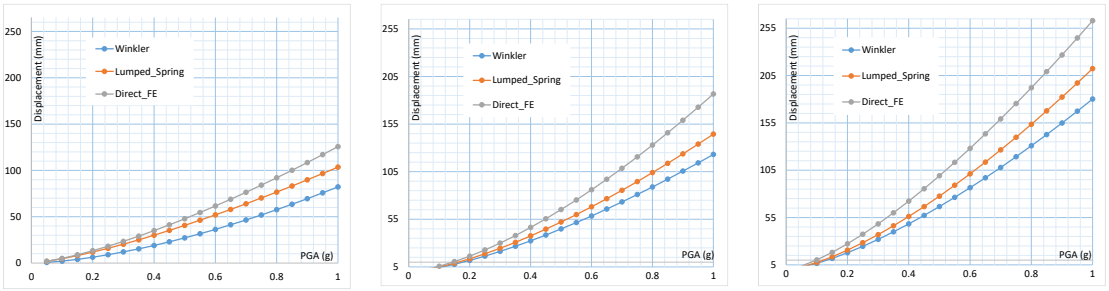

(a) Soil Profile #1 *(b) Soil Profile #2 – no liquefaction* *(c) Soil Profile #2 – liquefaction*

Figure 43: Bridge deck displacements

4.7 COMPUTATIONAL TIME AND EFFORT

One of the open questions that stills unanswered is how much it costs, on a relative basis, to jump from a simplified approach (e.g. Lumped spring model) to a more refined and accurate modelling (e.g. Direct FE model). This is quite relevant for decision makers (e.g. design offices and bridge owners) in order to better understand and decide on the most suitable approach, depending on the requirements for this.

Hence, Table 13 attempts to show a list of tasks that have been needed to carry-out along this work. Moreover, the time-periods that have been needed to be taken to complete them are also presented. These values have been recorded while conducting the structural analysis analyses. Of course that these values are dependent on the experience and capacity of the expert nevertheless, these are used as a real case that took place (i.e. along this work) and with the aim to take conclusions about the costs requirements vs. results accuracy / knowledge. In addition, a civil engineer's average hourly pay-rate of £ 17.50 (Payscale, 2018) in order to allow to convert the times invested to a monetary value.

Table 13: Tasks performed for each analysis and their required completion times

	TIME / EFFORT INVESTED FOR ANALYSIS (HOURS)		
TASK	**Lumped Spring**	**Winkler Spring**	**Direct FE Method**
Calculate p-y curves / soil parameters	-	2.0	1.0
Determine Pier spring constants	3.0	-	-
Determine Abutment spring constants	2.0	2.0	-
Build model in software	1.5	2.0	3.0
Test / Check model	1.5	1.5	2.5
Analysis run-times (x 50)	1.67	12.50	25.00
TOTAL	**9.67**	**20.00**	**31.50**

V. DISCUSSION OF RESULTS

5.1 INTRODUCTION

Further to the results presented in the previous section, a holistic discussion is herein performed with the clear objective in better understanding the influence of the soil-structure modelling approach in the fragility curves.

Firstly, a preliminary check related to the static and dynamic behaviour of the bridge is done in order to give evidence of the robustness of the FE model approach. Secondly, the fragility curves obtained at the bridge component level and the bridge system level are compared by depicting the results by the type of soils and SSI methods used in this work. Thirdly, an assessment is made against the case studies found in literature (outlined in section 2). The results obtained for the deck girder displacements, in relation to the employed SSI methods, are selected as the basis for this comparative analysis. Finally, an assessment between the quality of the obtained results, by the different levels of detail used in the modelling of the soil-structure interaction, and the monetary costs, associated with the time and resources needed to invest for each, is properly discussed towards the definition and quantification of requirements related to the structural analysis of bridges highly dependent on the soil-structure interaction.

5.2 ASSESSMENT OF THE STATIC AND DYNAMIC BEHAVIOUR

In order to assure the required robustness and accuracy of the FE models that have been developed, firstly. Some checks are done in terms of assessing the stiffness of the FE models at both levels, static and dynamic.

Hence, the static structural behaviour of the bridge is checked for the deflections due to the self-weight of the structure. For this, hand-calculations were done to calculate them, by referring to standard structural beam diagrams and formulas. More specifically, and for this case, the formula for 3-equal spans beam is used from the *American Institute of Steel Construction* (AISC) Manual of Steel Construction, as shown in Figure 44. Table 14 shows the calculations and the results obtained. As it can be observed, these results matches with the respective ones obtained by the Lumped-spring FE model, as showed in Figure 45.

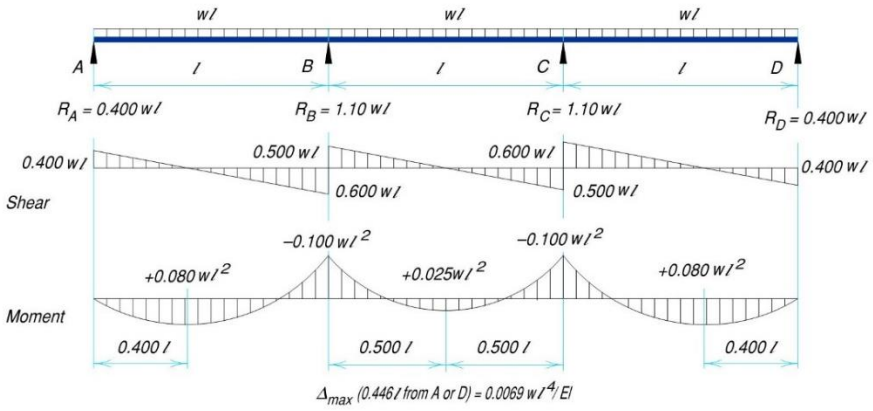

Figure 44: Beam diagram for a fully loaded continuous beam with three equal spans (AISC, 1994).

Table 14: Bridge deflections – hand calculations (AISC, 1994).

CALCULATE w (kN/m):							
γ_{conc} =	25.00	kN/m^3	Cross-sectional Area of Concrete slab, $A_{conc.}$ =			2.672	m^2
γ_{steel} =	76.98	kN/m^3	Cross-sectional Area of Steel beams, A_{steel} =			3.720	m^2
$w = \gamma_{conc.}A_{conc.} \times \gamma_{steel}A_{steel} =$						**353.17**	**kN/m**
DETERMINE 'E' and 'I' FROM SOFTWARE:							
$I_{deck\_section}$ =	**0.0021**	**m^4**					
E_{conc} =	3.5E+07	kN/m^2	E_{steel} =	2.0E+08	kN/m^2	E_s / E_c =	5.71
CALCULATE DEFLECTION (mm)							
l =	30.3	m	$\Delta_{max.} = 0.0069wl^4/EI =$			**2.4**	**mm**

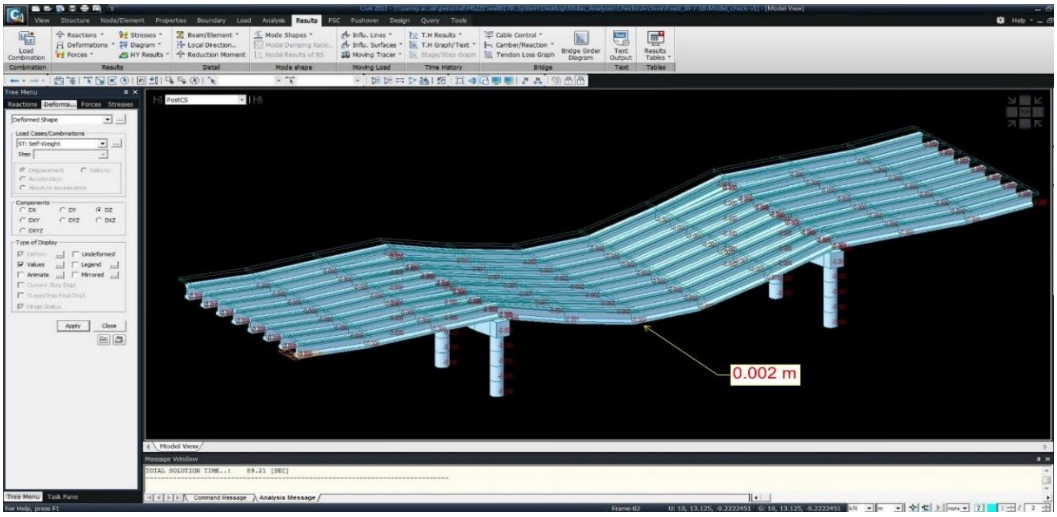

Figure 45: Bridge deflections – FE results (Civil MIDAS)

Additionally, the dynamic behaviour was also assessed. Mainly by checking the fundamental periods of the structure. According to the literature (i.e. standards on structural mechanics) indicates that this is a function of the stiffness and mass of the bridge under analysed. For this specific case, the periods for the first 5 modes of vibration were extracted and compared to the results from Nielson (2005), by taking

advantage that both bridges are similar (Table 15). As it can be observed, the results how that the dynamic behaviour are very similar for the first two periods, whereas for the remaining ones the differences increase. Indeed, and taking into account that higher modes are more sensitive to boundary conditions and/or changes in the structure stiffness, these differences might be explained by the improved and more accurate modelling of the soil-structure interaction.

Table 15: Fundamental periods related to the first 5 modes of vibration (sec).

Mode	Nielson (2005)	Wazeer (2018)	Difference
1st	0.2952	0.2910	-1.4 %
2nd	0.2535	0.2430	-4.1 %
3rd	0.2337	0.1630	-30.3 %
4th	0.1787	0.1092	-38.9 %
5th	0.1439	0.0847	-41.1 %

An additional check that has been done is to verify the values used for the soil springs. Nevertheless, these checks were already incorporated in the derivation and calculations for the p-y curves for both Lumped and Winkler springs. These calculations can be found in *Appendix B.*

5.3 ASSESSMENT OF THE BRIDGE COMPONENTS LEVEL

5.3.1 Influence of the Type Of Soil

Firstly, the influence of the type of soil, i.e. (i) Soil #1, (ii) Soil #2 without liquefaction and (iii) Soil #2 with liquefaction, on the fragility curves for the different bridge components is discussed. For this, the results presented in Sections 4.3.1, 4.4.1 and 4.5.1 are used as bottom line and further to them the following can be stated.

- **Soil profile #1:**

This soil profile leads to the lowest probabilities of failure for all the bridge components. Indeed, the plotted results for this soil are approximately 10% and 30% lower than Soil #2 without liquefaction and with liquefaction, respectively. This can be explained by the higher stiffness properties, as determined in *Section 3.5,* in relation to the p-y curves, shear modulus and other correlated parameters.

- **Soil profile #2: Without liquefaction**

This soil profile leads to slightly higher probabilities of failure than Soil #1, although the differences are almost negligible at the 'Slight damage' limit state. The calculated p-y curves and subsequent stiffness for this soil were slightly less than Soil #1.

- **Soil profile #2: With liquefaction**

As expected, this soil profile leads to the highest probabilities of failure for all the bridge components. This is explained by the small soil-resistance, due to the liquefaction, which is reflected in the low spring-stiffness values and near-zero effective stress used to model this soil profile.

To support these conclusions, Figure 46 shows two set of results related to two different bridge components, mainly a column and a rocker bearing, where it is evident that despite the soil-structure interaction method used, larger differences are still observed between different soil profiles as the damage severity increases from moderate to complete. It can be seen that the effect applies to any of the bridge components and with any SSI method used.

Hence, it becomes clear that the type of soil holds an increasing importance on the fragility of the bridge components as the damage increases, and mainly, when the soil liquefaction occurs.

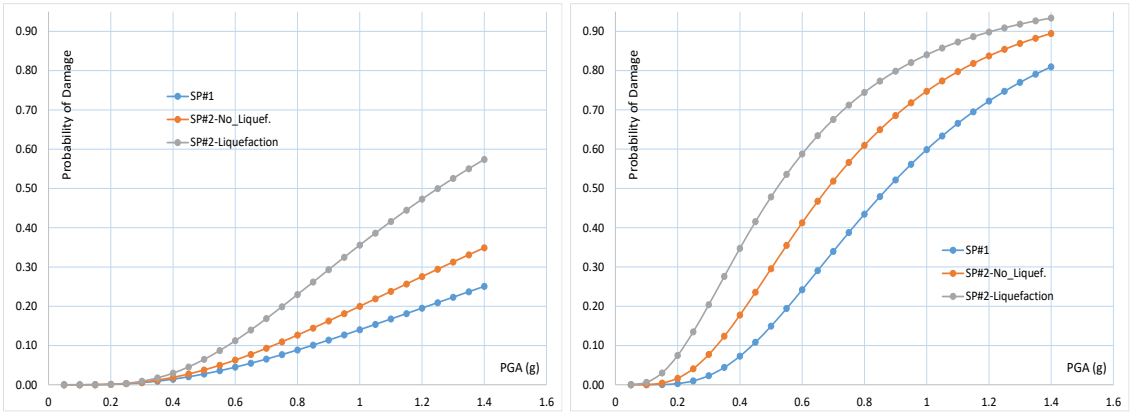

(a) Complete – Column (Winkler Spring) *(b) Moderate – Rocker bearing (Direct FE)*

Figure 46: Comparison of bridge component fragilities based on the type of soils

5.3.2 Influence of the SSI Approach

Secondly, the influence of the type of SSI approach used, i.e. (i) Winkler Spring method, (ii) Lumped spring method and (iii) Direct FE modelling method, on the

fragility curves for the different bridge components is also discussed. For this, the results presented in Sections 4.3.1, 4.4.1 and 4.5.1 are used as bottom line and further to them the following can be stated.

- **Winkler Spring method**

By using this method, the probabilities of failure for the Rocker-bearing and Abutment components are found to be the lowest, with differences ranging from 10% to 25% lower, for the Rocker-bearing, and 15% to 35%, for the Abutment, in relation to the Lumped-spring and Direct FE methods respectively. This method leads to slightly lower results, when compared to the Lumped Spring method for the Column and Fixed-bearing components. This can be explained by the fact that this method models the full piles for the pier foundation instead of single point-springs as used in the lumped-spring method.

- **Lumped Spring method:**

This method leads to the highest probabilities of failure for the Column and Fixed-bearing components. The differences range from 7% to 15% higher, for the column, and 10% to 30% higher, for the fixed-bearing (depending on the type of soil and level of damage), in relation to the Winkler-spring and Direct FE methods respectively. This can be explained by the fact that the pier foundations are being modelled as single lumped-springs instead of the more refined models used in the other two methods.

- **Direct Method:**

This method leads to the highest probabilities of failure for the Abutment and Rocker-bearing components, with differences ranging from 20% to 35% higher for the Abutment and 10% to 20% for the Rocker-bearing, in relation to the Lumped-spring and Winkler-spring methods respectively. It also leads to the lowest values for the Column and Fixed-bearing components, with similar differences as stated above in the Lumped spring model.

It is worth to note that these higher probabilities, for the Abutment and Rocker-bearing components, can be explained by the approach how forces/pressures from the soil-finite elements act on the abutments in this case, as opposed to the other two models where the effect of the soils is simply simulated by springs. Moreover, the differences can also be explained by the consideration of additional parameters in this case to

define the soil properties in the Direct FE model and how these parameters are correlated to empirical data i.e. the shear modulus and Poisson's ratio used for this method may not exactly match to the spring stiffness used in the other models because of the very nature of the correlation tables.

Table 16 synthetizes the above conclusions by highlighting which SSI approach lead to the lowest and highest probability of failures obtained for the different bridge components. This summary reveals that if one is considering the individual components of a bridge, in terms of making decisions for retrofitting, the SSI method used for analysis has a significant impact on the fragility results. As a simple but very informative example: the decision-maker with responsibilities in bridge management could see that there is a 60% probability of failure for a rocker bearing if the Winkler method is used, although this can be in reality (i.e. based on more accurate analysis such as the Direct method) of 80% probability.

Table 16: Comparison of component fragility in relation to SSI method of analysis

	Column/Pier	**Fixed bearings**	**Rocker bearings**	**Abutments**
Highest probability of failure	Lumped Spring	Lumped Spring	Direct FE Method	Direct FE Method
	Winkler Spring	Winkler Spring	Lumped Spring	Lumped Spring
Lowest probability of failure	Direct FE Method	Direct FE Method	Winkler Spring	Winkler Spring

5.4 ASSESSMENT AT BRIDGE SYSTEM

5.4.1 Influence of the Type Of Soil

Firstly, the influence of the type of soil, i.e. (i) Soil #1, (ii) Soil #2 without liquefaction and (iii) Soil #2 with liquefaction, on the fragility curves for the different bridge components is discussed. For this, the results presented in Sections 4.3.3, 4.4.3 and 4.5.3 are used as bottom line and further to them the following can be stated.

Hence, it should be noted that in graphical results, some of the components have higher probabilities of failure than the whole bridge system itself (depending on the SSI method and level of damage). However, it can still be seen, as illustrated in Figure 47 , that similar to how the type of soils affect the bridge components, the effect propagates into the whole bridge system. This leads to the conclusion that the type of soil affects the bridge system in a very similar way as it affects the individual bridge components.

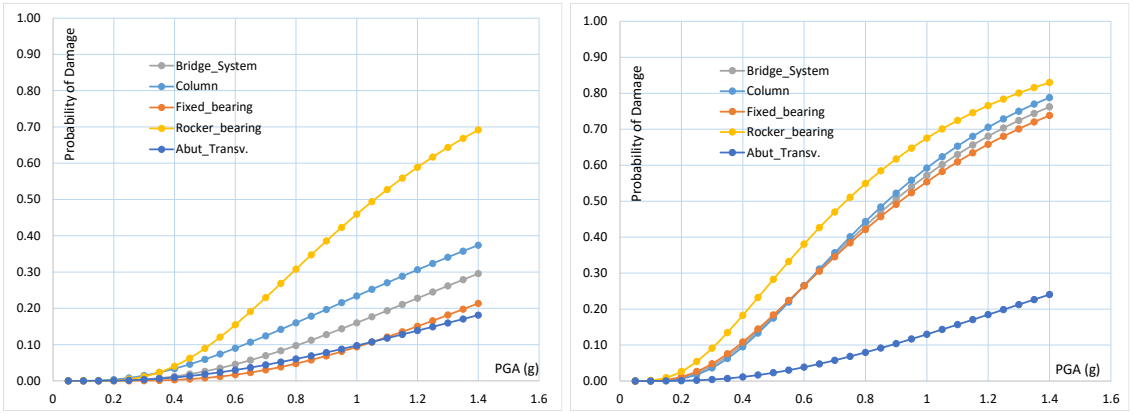

(a) Soil #1 (Direct FE) *(b) Soil #2 with liquefaction (Direct FE)*

Figure 47: Bridge components vs. bridge system fragilities for Extensive damage.

In addition, Figure 48 shows that for the level of Slight damage, the probabilities of failure based on the type of soils are basically the same and could be considered negligible. The differences are more prominent from moderate to complete levels of damage.

This leads to the conclusion that, at the bridge system level, the type of soil has more significant impact when higher levels of damage are considered i.e. moderate to complete damage.

5.4.2 Influence of the SSI Approach

Secondly, the influence of the type of SSI approach used, i.e. (i) Winkler Spring method, (ii) Lumped spring method and (iii) Direct FE modelling method, on the fragility curves for the different bridge components is also discussed. For this, the results presented in Sections 4.3.2, 4.4.2 and 4.5.2 are used as bottom line and further to them the following can be stated.

As a main conclusion, it can be stated that the Lumped spring method leads, generally, to the highest probabilities of failure, followed by the Winkler method. The Direct FE method leads to the lowest probabilities of failure, despite the fact of leading to the highest values for the individual components (e.g. Rocker-bearings and Abutments, Section 5.2.2). This could be due to its low probabilities of failure for all the other bridge components.

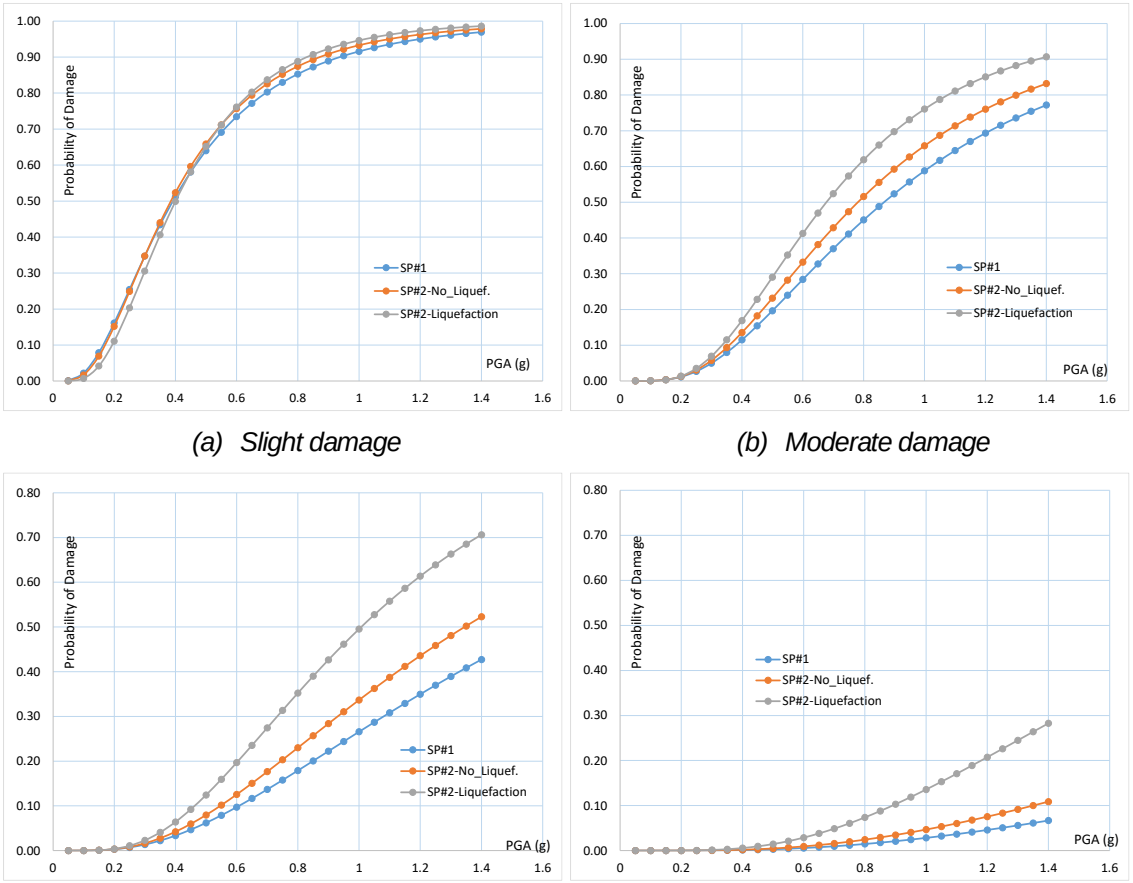

(a) Slight damage *(b) Moderate damage*

(c) Extensive damage *(d) Complete damage*

Figure 48: Bridge system fragilities vs. type of soil – Winkler Spring method.

5.5 ASSESSMENT AGAINST THE CASE STUDIES IN THE LITERATURE

Although a complete comparison to any of the case studies found in the literature and mentioned in this work would be difficult to be done, due to different ground motions and soil profiles mainly, some comparisons are made in some relevant issues. The reason for this is related to the similarity of the case study selected with the respective ones.

- **Aygun et. al (2010)**

Aygun et. al (2010) analysed how liquefaction affects the probabilities of damage to the bridge components. Their measured increase in probability due to liquefaction is similar to the results of this report. As shown in Figure 49, when liquefaction is considered, their probability of damage increased by approximately 20% for the 1st bent column. Taking into account the Winkler-spring approach used, indeed, this has been also observed for the case study analysed in this work (Figure 49).

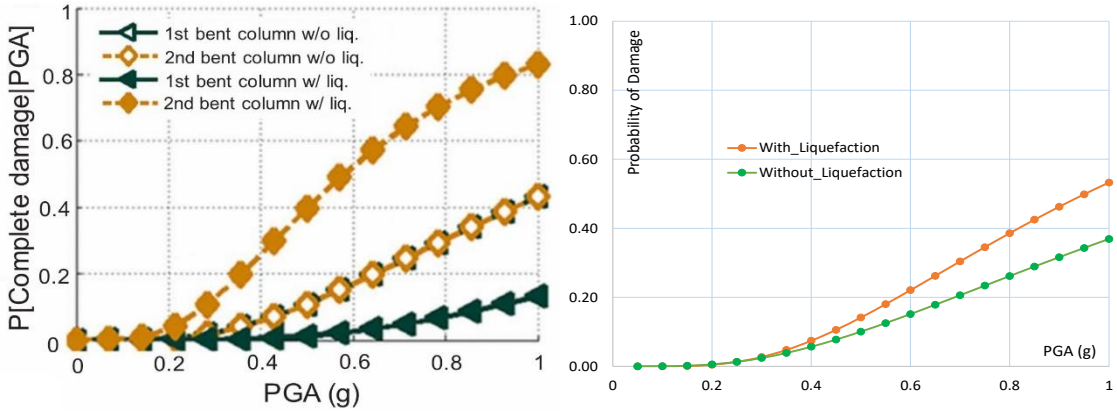

(a) Aygun et. al (2010) *(b) Soil Profile #2 – Winkler spring*

Figure 49: Comparison of column liquefaction effects.

- **Stefanidou et. al (2017)**

Although Stefanidou et. al (2017) did not study the same bridge type, they observed that the abutment components had higher damage probabilities when detailed SSI analyses are used compared to simpler methods of analyses. Indeed, the same pattern is observed in this work, where the abutments have higher probabilities of damage with Direct FE method, when compared to the other two methods.

As shown in Figure 50 (a), for each increasing level of damage limit states (LS1 to LS4) the detailed SSI analysis (i.e. 'SSI full') is higher than simplified SSI analysis. Similarly, in (b) the detailed SSI analysis using the Direct FE method has higher probabilities at every level of damage.

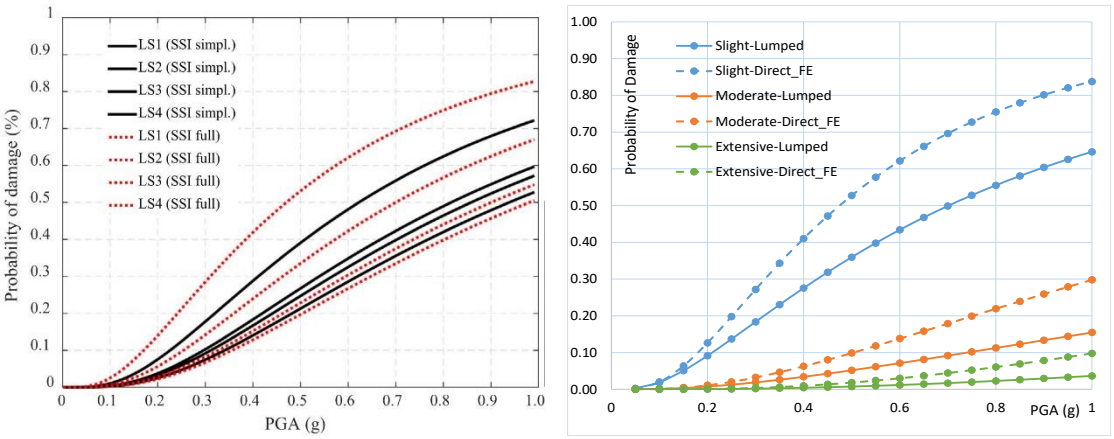

(a) Stefanidou et. al (2017) *(b) Soil Profile #1*

Figure 50: Comparison of abutment fragilities based on detailed SSI analysis.

- **Zong (2015) and Nielson (2005)**

Zong (2015) concluded that the probabilities of failure for both the bridge system and components decreased when SSI effects are included. Although the findings of this report agree with Stefanidou et. al (2017) on the bridge components, it was shown in Section 5.2.2 that the Direct-FE method, which is the most detailed and refined approach, had the lowest values in all analyses of the whole bridge system. Hence this report agrees with Zong (2015) in the context of the whole bridge system. However, since the soil profiles, ground motions and component assembly for the bridge system are different, a direct comparison cannot properly be made.

With respect to Nielson (2005), comparisons were made to the structural periods (Section 5.2). But the fragility curves from both reports do not match because of the same reasons mentioned above, i.e. different ground motions and soil types.

5.6 ASSESSMENT OF THE DECK GIRDER DISPLACEMENTS

From a structural point of view, as the FE model approach becomes more refined and detailed (i.e. by incorporating more information from the real conditions in the field), the respective results are expected to be more accurate and reliable and therefore, less conservative values. This becomes of high relevance when problems due to malfunctioning of the bridge becomes critical such as the case of bearings and joint devices. Hence, this means that if more refined analysis is used, one can expect to save, in turn, on the design/replacement of such devices with more reliable and representative displacement ranges.

In this context, a comparative analysis is also performed in terms of the expected magnitude of displacements for the different SSI modelling approaches explored in this work. Figure 51 summarizes the deck girder displacements obtained for the different soil profiles explored and by using the Direct FE approach. It can clearly be seen that the Direct FE method produces greater displacements of the bridge deck, which would be the more conservative results. The differences in these deck displacements range from 40mm in Soil #1 to 90mm for liquefaction effects in Soil #2. This translates to a 50% increase in displacement for both instances. Therefore in this report, the more refined analyses show that one would have to spend more on bearings that allow for a greater range of movement.

From Section 5.6 it can also be observed that the type of soils also affect the bridge deck displacements. Figure 51 shows that the maximum deck displacement for Soil #2 is 60 mm higher than Soil #1 and with liquefaction effects, it is 137 mm higher. This also translates to a 48% and 100% increase respectively.

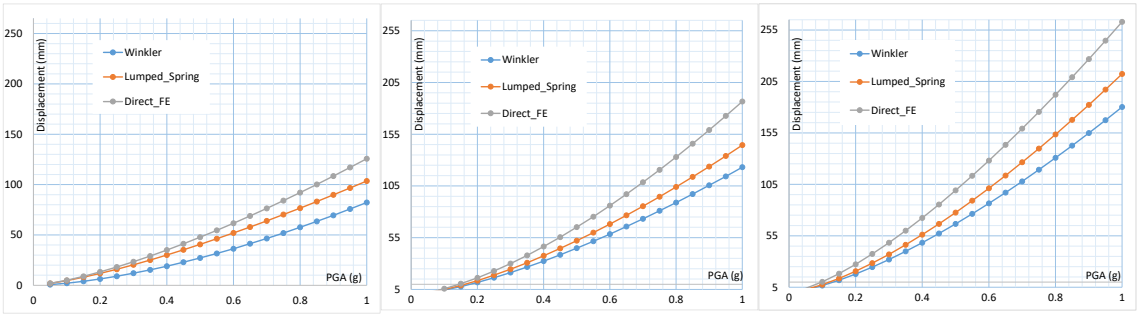

Soil Profile #1 *Soil Profile #2 – no liquefaction* *Soil Profile #2 – liquefaction*

Figure 51: Comparison of bridge deck displacements in terms of Soil type

Therefore, the findings of this report show that the SSI method used for analysis has approximately the same effect on deck displacements as the type of soil used in the analysis i.e. about 50% increase/decrease depending on the choice. The exception to this would be in the case of liquefaction where the displacements are basically doubled in value.

5.7 COSTS ANALYSIS ASSOCIATED WITH THE SSI APPROACHES

Further to the cost model presented in the previous section (Chapter 4), and based on the analysis preformed in this work, Table 17 summarizes the results obtained by depicting the type of SSI approach. Details are given in terms of probabilities of damage, either at the bridge component level or the bridge system level, and displacements of the deck girder. The associated monetary costs are outlined in the last column.

Straightforwardly, the costs associated in developing a comprehensive, refined and representative of the bridge (i.e. the Direct FE model) is approximately 3 times higher than the simplest approach (i.e. the Lumped Spring) and the double of a more elaborated approach for the SSI (i.e. Winkler spring). Hence, and in a first instance, the decision maker becomes very clear about how much it costs to move from one

level to the following one, in terms of costs, in addition to the already expected improvement on the results accuracy.

Nevertheless, the most important information perhaps is to better understand, and inform the decision maker, where the marginal investment made will be capitalized.

Hence, an approach based on the most expensive analysis (i.e. the Direct FE method), is mainly worthwhile if the problem on the bridge is related to the bearings/joint devices (e.g. their replacement) or if the criticality of the bridge under analysis is high (e.g. the London Bridge) and its failure as a system holds a huge impact in a socio-economic perspective. On the contrary, for a bridge located somewhere in the countryside perhaps the investment on a refined SSI analysis is not capitalized properly.

On the contrary, an approach based on the less expensive approach (i.e. the Lumped spring method), is mainly worthwhile if the criticality of the bridge is not so high. The fragility results obtained for both bridge component and bridge system are the highest among the three methods herein analysed. This means that the option for a lower investment in the FE approach is only acceptable if the additional costs in terms of materials placed in situ and/or the consequences of a failure is not critical.

Finally, the Winkler method seems to be the most cost-effective approach, by providing satisfactory results for both fragilities and displacements.

Table 17: Comparison of the results achieved to the costs associated with each analysis

FINITE ELEMENT APPROACH	Probability of Component Damage / Fragility	Probability of Bridge system Damage / Fragility	Bridge Deck Displacement	Total Time Investment (hrs.)	Time * hourly rate of £17.50
Lumped Spring	Highest: columns & bearings	Highest	*middle values*	9.67	£ 169.17
Winkler Spring	*middle values*	↑	least conservative	20.00	£ 350.00
Direct FE Method	Highest: abutments	Lowest	most conservative	31.50	£ 551.25

Of course, that the decision in opting for a SSI approach depends on several factors and not only on the ones mentioned in this report. Nevertheless, it is also important to quantify these costs associated with the development of different type of FE models in order to rationally and efficiently decide the best approach for each case.

VI. CONCLUSIONS AND FUTURE WORK

6.1 CONCLUSIONS

This report aimed to discuss how different SSI affects the structural seismic response of a bridge type widely used in transportation networks – MSC Steel Girder bridge. More specifically, and according to the advancements on the state-of-the-art, three SSI methods were explored, mainly: (i) the Lumped-spring method, (ii) the Winkler-spring method and (iii) the Direct Finite Element method. In addition, two different typical sites were considered, with one of them showing potential of liquefaction. In addition, a cost-benefit analysis was done.

More specifically, and according to the main tasks outlined in Section 2.5, the following was achieved:

- Probabilities of a bridge failure were compared based on different soil profiles or sites,
- The probabilities were also compared based on SSI modelling methods used for analyses,
- Bridge deck displacement results from the varying SSI analyses were compared,
- The costs associated with the different analyses were related to the results achieved.

Based on this, it has been found that the SSI modelling approach holds a significant impact on the bridge component fragility, with differences up to 20 % depending on the SSI method used. Moreover, it has been found that this is mainly critical at the component level, whereas the impact of the SSI approach at the bridge system level holds a smaller impact in terms of results' differences. Nevertheless, it has also been concluded that, as expected, the type of soil affects the bridge fragility when higher levels of damage are considered. Hence, it becomes evident that by considering or not the real in-situ conditions with a more or less refined SSI approach leads to completely different results, at both bridge component level and bridge system level, which becomes more critical (i.e. in terms of differences) as the damage level increases.

Despite of this, it could be concluded that a more refined model is always better. Nevertheless, this might not be completely correct from a cost-benefit perspective,

which is something highly relevant for decision makers. Indeed, although the most refined model – Direct FE analysis – may produce more accurate results for the bridge system fragility, more conservative values are obtained for some components such as bearings and abutments due to forces acting on them from the soiled modelled as linear-strain elements as opposed to springs. On the other hand, the Lumped spring method produces the most conservative results overall.

Hence, and mainly towards decision-makers, the following main conclusions can be drawn:

- The derivation of fragility curves needs to be performed on a more holistic approach. Practically speaking, this should also be based on Site Class in addition to Bridge Class. For example, in a transportation network, the same type of bridge class should have a different fragility curves based on its site-type and/or location within the network,
- The SSI modelling approach has a higher impact on the bridge component fragility, when compared to the bridge system fragility. This can be a critical criterion if retrofitting decisions are needed to be taken,
- The utilization of more refined SSI analyses may not necessarily result in more economical design/assessment, mainly bearings and joint devices. This is showed in terms of the bridge deck displacements derived by the different SSI methods used,
- An organisation may achieve satisfactory results with conventional analysis methods such as Winkler springs, as far as the socio-economic impact of abnormal behaviour of a bridge is moderate (e.g. closure after a seismic event). Nevertheless, if a specific bridge holds a high level of criticality within a transportation network (e.g. London Bridge), then the additional costs associated with a more refined method (e.g. Direct FE method) may be justifiable by the savings that this might bring in catastrophic scenarios (i.e. more suited for high-risk projects which may result in litigation).

6.2 FURTHER STEPS AND FUTURE WORK

At this stage, the author envisages the following 5 items that can be explored in future work, on the basis of a better understanding and improve the reliability of the conclusions outlined above:

- The effects of sloped layers in the soil profile should be considered in the SSI modelling, as opposed to perfectly horizontal layers,
- A wider range of the bridge component/system limit states should be utilized in this type of analyses, instead of just the 8 components that are explored in this report,
- Other bridge classes should also be analysed by using the approach/methods that have been employed in this report to MSC Steel Girder bridge,
- Other standards, in complement to Eurocodes, should be explored and assess the differences to further a better comprehension of the SSI modelling,
- The framework, i.e. the approach and methods presented in this report, is not restricted to bridges. Indeed, this can be used for any type of Civil Engineering structures where the SSI is a key element, for instance buildings.

REFERENCES

AISC, L., 1994. Manual of steel construction, load and resistance factor design.

Alp Oasys Pile Version 19.6., 2017, Oasys Inc., London, United Kingdom.

API, R., 2A-WSD 21st Edition, 2000. *Recommended Practice for Planning, Designing, and Constructing Fixed Offshore Platform, American Petroleum Institute, Washington DC*.

Aygün, B., Dueñas-Osorio, L., Padgett, J.E. and Des Roches, R., 2010. Efficient longitudinal seismic fragility assessment of a multi-span continuous steel bridge on liquefiable soils. Journal of Bridge Engineering, 16(1), pp.93-107.

BBFL Consultants Ltd., 2016. *North Sangre Grande Interchange - Churchill Roosevelt Highway Extension to Manzanilla*. Ministry of Works and Transport, Trinidad and Tobago.

Bhattacharya, S., Tokimatsu, K., Goda, K., Sarkar, R., Shadlou, M. and Rouholamin, M., 2014. Collapse of Showa Bridge during 1964 Niigata earthquake: A quantitative reappraisal on the failure mechanisms. *Soil Dynamics and Earthquake Engineering*, *65*, pp.55-71.

Bowers, M.E., 2007. Seismic fragility curves for a typical highway bridge in Charleston, SC considering soil-structure interaction and liquefaction effects (Doctoral dissertation, Clemson University).

Brown, D.A. and Reese, L.C., 1988. *Behavior of a large-scale pile group subjected to cyclic lateral loading*. TEXAS UNIV AT AUSTIN GEOTECHNICAL ENGINEERING CENTER.

Caltrans, S.D.C., 2010. Caltrans seismic design criteria version 1.6. *California Department of Transportation, Sacramento*.

Chang, Liang & Elnashai, Amr & Spencer, Billie. (2012). Post-earthquake modelling of transportation networks. Structure and Infrastructure Engineering. 8. 893-911. 10.1080/15732479.2011.574810.

Choi, E., DesRoches, R. and Nielson, B., 2004. Seismic fragility of typical bridges in moderate seismic zones. *Engineering Structures*, *26*(2), pp.187-199.

Code, P., 2005. Eurocode 8: Design of structures for earthquake resistance-part 1: general rules, seismic actions and rules for buildings. *Brussels: European Committee for Standardization*.

Cornell, C.A., Jalayer, F., Hamburger, R.O. and Foutch, D.A., 2002. Probabilistic basis for 2000 SAC federal emergency management agency steel moment frame guidelines. *Journal of structural engineering*, *128*(4), pp.526-533.

Dash, S., Rouholamin, M., Lombardi, D. and Bhattacharya, S., 2017. A practical method for construction of py curves for liquefiable soils. *Soil Dynamics and Earthquake Engineering*, *97*, pp.478-481.

ENGM054 Earthquake Engineering, 2018. *UNIT 6 Engineering Correlations for Seismic Design of Foundations*. PG Cert/PG Diploma/MSc. University of Surrey

Karamlou, A., & Bocchini, P. (2015). Computation of bridge seismic fragility by large-scale simulation for probabilistic resilience analysis. Earthquake Engineering & Structural Dynamics, 44(12), 1959-1978.

Kawashima, K., Unjoh, S., Hoshikuma, J.I. and Kosa, K., 2011. Damage of bridges due to the 2010 Maule, Chile, earthquake. *Journal of Earthquake Engineering*, *15*(7), pp.1036-1068.

Kudo, K., Uetake, T. and Kanno, T., 2000. Re-evaluation of nonlinear site response during the 1964 Niigata earthquake using the strong motion records at Kawagishi-cho, Niigata City. In *Proc 12th World Conf Earthq Eng* (No. 0969). http://smsd.eri.u-tokyo.ac.jp/smad/?action_1964niigata=true

Kwon, O.S. and Elnashai, A., 2006. The effect of material and ground motion uncertainty on the seismic vulnerability curves of RC structure. *Engineering structures*, *28*(2), pp.289-303.

Kwon, O. and Elnashai, A.S., 2008. Multi-platform simulation of highway over-crossing bridge with consideration of soil–structure interaction. *Journal of Structural Engineering, ASCE*, *134*(4), pp.651-660.

Kwon, O.S., Sextos, A. and Elnashai, A., 2009, September. Seismic fragility of a bridge on liquefaction susceptible soil. In *10th international conference on seismic safety and reliability* (pp. 13-17).

Kwon, O.-S. & Elnashai, A. S. (2010) Fragility analysis of a highway over-crossing bridge with consideration of soil–structure interactions. *Structure and Infrastructure Engineering*, 6(1-2), 159-178.

Lombardi, D., & Bhattacharya, S. (2016). Evaluation of seismic performance of pile-supported models in liquefiable soils. Earthquake Engineering & Structural Dynamics, 45(6), 1019-1038.

Lombardi, D., Dash, S.R., Bhattacharya, S., Ibraim, E., Wood, D.M. and Taylor, C.A., 2017. Construction of simplified design py curves for liquefied soils. *Geotechnique*, *67*(3), pp.216-227.

Mander, J.B., Kim, D.K., Chen, S.S. and Premus, G.J., 1996. *Response of steel bridge bearings to reversed cyclic loading*(No. NCEER-96-0014).

MATLAB and Statistics Toolbox Release 2017, The MathWorks, Inc., Natick, Massachusetts, United States.

Mylonakis, G., Nikolaou, S. and Gazetas, G., 2006. Footings under seismic loading: Analysis and design issues with emphasis on bridge foundations. *Soil Dynamics and Earthquake Engineering*, *26*(9), pp.824-853.

Nielson, B.G., 2005. Analytical fragility curves for highway bridges in moderate seismic zones (Doctoral dissertation, Georgia Institute of Technology).

Nielson, B.G. and DesRoches, R., 2007. Seismic fragility methodology for highway bridges using a component level approach. *Earthquake Engineering & Structural Dynamics*, *36*(6), pp.823-839.

PayScale, 2018. Civil Engineer Salary. https://www.payscale.com/research/UK/Job=Civil_Engineer/Salary [Accessed 17 August, 2018]

Pecker, A., & International Centre for Mechanical Sciences. (2007). Advanced Earthquake Engineering Analysis (CISM International Centre for Mechanical Sciences, 494). Wien ; New York: Springer.

Sextos, A.G., Pitilakis, K.D. and Kappos, A.J., 2003. Inelastic dynamic analysis of RC bridges accounting for spatial variability of ground motion, site effects and soil–structure interaction phenomena. Part 1: Methodology and analytical tools. *Earthquake engineering & structural dynamics*, *32*(4), pp.607-627.

Stefanidou, S.P. and Kappos, A.J., 2017. Methodology for the development of bridge-specific fragility curves. *Earthquake Engineering & Structural Dynamics*, *46*(1), pp.73-93.

Stefanidou, Sextos, Kotsoglou, Lesgidis, & Kappos. (2017). Soil-structure interaction effects in analysis of seismic fragility of bridges using an intensity-based ground motion selection procedure. Engineering Structures, 151, 366-380

Zirakian T, Boyajian D (2016) Recent Studies on Steel Plate Shear Wall Systems. J Steel Struct Constr 2:e104. doi:10.4172/2472-0437.1000e104

Zong, X., 2015. Seismic fragility analysis for highway bridges with consideration of soil-structure interaction and deterioration. City University of New York.

APPENDIX A: SCALED GROUND MOTION RECORDS

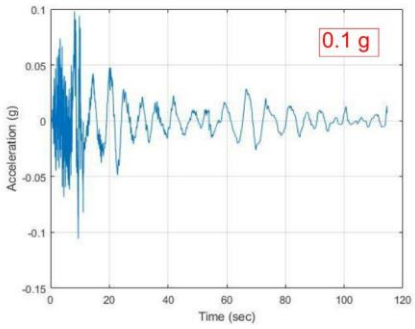

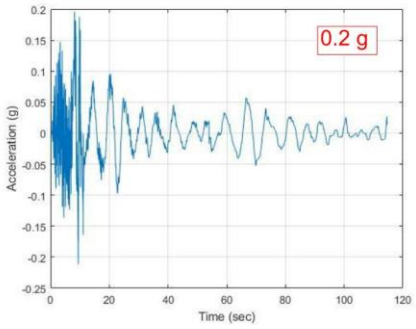

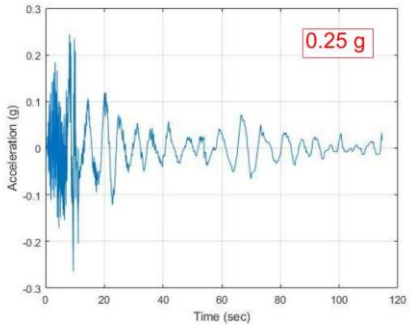

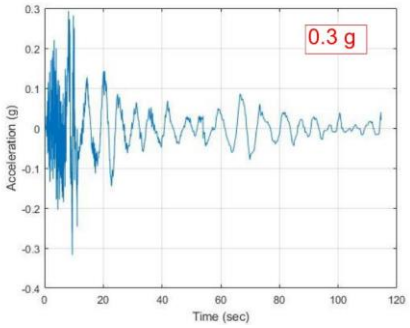

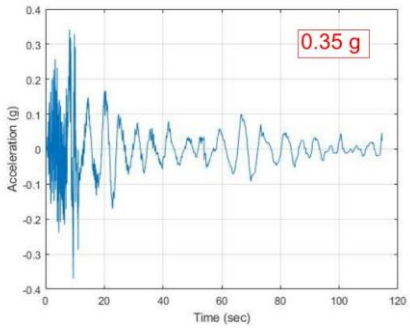

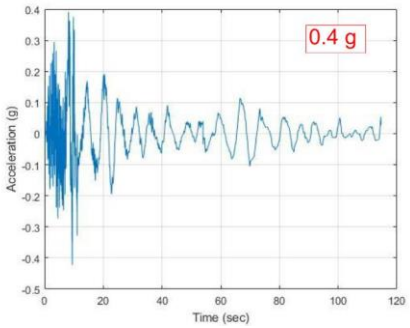

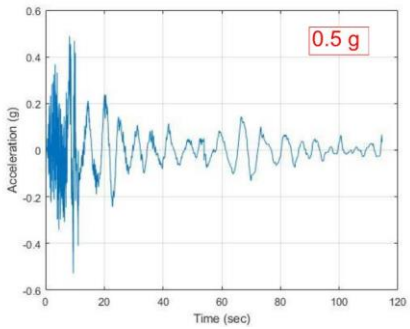

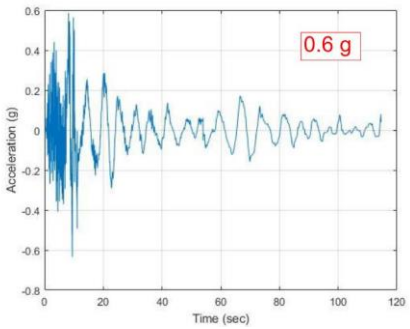

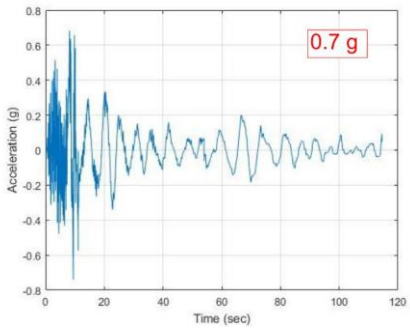

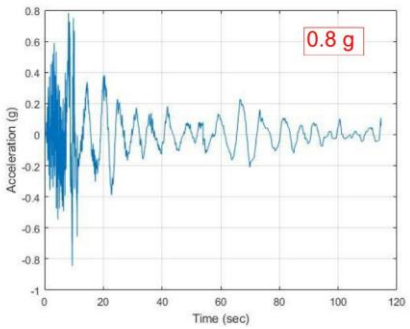

(Scaled in order from 0.1g to 0.8g)

APPENDIX B: CALCULATION OF P-Y CURVES (LIQUEFIABLE SOILS)

Soil depth, d = 5 m γ_{water} = 9.81 kN/m^3

SPT, N = 5 blows

γ_{soil} = 17 kN/m^3

$\sigma'_v = d \times (\gamma_{soil} - \gamma_{water}) =$ 35.95 kPa

SPT value corrected for overburden = $N_1 = {}^{N}/_{\sqrt{\sigma'_v/98}} =$ 8 blows

Effective confining stress = $p_{ini}{}' = {}^{2}/_{3} \times \sigma'_v =$ 23.97 kPa

C_D = 20 (sand with fines)

41 (clean sand)

70 (gravelly sand)

Relative density of soil = $D_r = \sqrt{{}^{N_1}/_{C_D}} =$ 44.2%

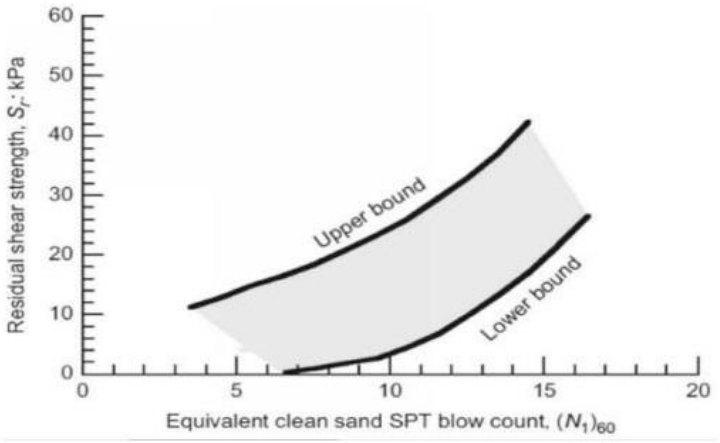

For N_1 = 8

(lower bound) s_u = 1.8 kPa

(upper bound) s_u = 20 kPa

$= \tau_{max}$

Pile Ø, D = 0.6 m

Pile material = steel (smooth interface)

Stress scaling factor, N_s = 9.2 (smooth) Strain scaling factor, M_s = 1.87

11.94 (rough) (fully liquefied soil)

Take off strain = $\gamma_{to} = 74.34 - 17.71 \ln(D_r) =$ 7.25%

Initial shear modulus = $G_1 = {}^{1}/_{\gamma_{to}} =$ 13.79 kPa

$G_{max} = 14400N^{0.68} =$ 43,019.18 kPa

Critical shear modulus = $G_2 = \frac{G_{max}}{5\sqrt{p_{ini}{}'}} =$ 1,757.47 kPa

P-Y CURVE PARAMETERS

Initial lateral resistance = $p_1 = N_s 1.25\gamma_{to} G_1 D =$ 6.9 kPa

Initial lateral displacement = $y_1 = \frac{1.25\gamma_{to} D}{M_s} =$ 0.0291 m

Ultimate lateral resistance = $p_u = N_s \tau_{max} D$

Lower bound = 9.94 kN/m

Upper bound = 110.40 kN/m

Ultimate lateral displacement = $y_u = \left(1.25\gamma_{to} + \frac{\tau_{max} - (G_1 1.25\gamma_{to})}{G_2}\right) \times \frac{D}{M_s}$

Lower bound = 0.0292 m

Upper bound = 0.0325 m

SMOOTHED P-Y CURVE

$$\omega = \frac{1}{2}\left[1 - \tanh\left(\frac{6\pi}{y_u}\left(y - \frac{4y_1 + y_u}{6}\right)\right)\right]$$

A = 0 for y = 0

1 for y not = 0

$$p = \omega\frac{p_1}{y_1}y + A(1-\omega)\left[\frac{p_u + p_1}{2} + \frac{p_u - p_1}{2}\tanh\frac{2\pi}{3(y_u - y_1)}\left(y - \frac{y_u + y_1}{2}\right)\right]$$

LOWER BOUND		
y (m)	ω	p (kN/m)
0	1.00E+00	0.00
0.0025	1.00E+00	0.59
0.005	1.00E+00	1.19
0.0075	1.00E+00	1.78
0.01	1.00E+00	2.37
0.0125	1.00E+00	2.97
0.015	1.00E+00	3.56
0.0175	1.00E+00	4.15
0.02	9.96E-01	4.76
0.0225	9.06E-01	5.62
0.025	2.77E-01	7.72
0.0275	1.49E-02	8.39
0.03	6.00E-04	8.42
0.0325	2.38E-05	8.42
0.035	9.42E-07	8.43
0.0375	3.73E-08	8.43
0.04	1.48E-09	8.43
0.0425	5.85E-11	8.44
0.045	2.32E-12	8.44
0.0475	9.16E-14	8.45
0.05	3.61E-15	8.45
0.0525	1.67E-16	8.45
0.055	0.00E+00	8.46
0.0575	0.00E+00	8.46
0.06	0.00E+00	8.46

UPPER BOUND		
y (m)	ω	p (kN/m)
0	1.00E+00	0.00
0.0025	1.00E+00	0.59
0.005	1.00E+00	1.19
0.0075	1.00E+00	1.78
0.01	1.00E+00	2.37
0.0125	1.00E+00	2.97
0.015	1.00E+00	3.56
0.0175	1.00E+00	4.16
0.02	9.96E-01	4.95
0.0225	9.36E-01	8.73
0.025	4.45E-01	35.01
0.0275	4.24E-02	56.28
0.03	2.43E-03	58.48
0.0325	1.34E-04	58.73
0.035	7.39E-06	58.87
0.0375	4.07E-07	59.00
0.04	2.24E-08	59.13
0.0425	1.24E-09	59.26
0.045	6.80E-11	59.38
0.0475	3.75E-12	59.51
0.05	2.07E-13	59.64
0.0525	1.13E-14	59.77
0.055	5.55E-16	59.90
0.0575	0.00E+00	60.03
0.06	0.00E+00	60.16

APPENDIX C: PSDM FOR THE BRIDGE COMPONENTS

SOIL PROFILE #1

Lumped Spring Method

Response [ln (S_d)]	PSDM						$\beta_{D\|PGA}$
	a			*b*			
ln (μ_φ)	ln	2.70	+	0.94	*	ln (PGA)	0.39
ln (fx_L)	ln	29.30	+	0.91	*	ln (PGA)	0.53
ln (fx_T)	ln	1.44	+	2.07	*	ln (PGA)	0.50
ln (ex_L)	ln	103.54	+	1.35	*	ln (PGA)	0.64
ln (ex_T)	ln	1.61	+	3.22	*	ln (PGA)	0.94
ln (ab_P)	ln	16.16	+	1.04	*	ln (PGA)	0.47
ln (ab_A)	ln	0.57	+	0.52	*	ln (PGA)	0.57
ln (ab_T)	ln	13.46	+	0.90	*	ln (PGA)	0.48

Winkler Spring Method

Response [ln (S_d)]	PSDM						$\beta_{D\|PGA}$
	a			*b*			
ln (μ_φ)	ln	2.34	+	0.90	*	ln (PGA)	0.37
ln (fx_L)	ln	23.79	+	1.04	*	ln (PGA)	0.56
ln (fx_T)	ln	1.52	+	1.99	*	ln (PGA)	0.52
ln (ex_L)	ln	82.27	+	1.60	*	ln (PGA)	0.75
ln (ex_T)	ln	1.69	+	3.09	*	ln (PGA)	0.97
ln (ab_P)	ln	16.97	+	1.00	*	ln (PGA)	0.49
ln (ab_A)	ln	0.60	+	0.50	*	ln (PGA)	0.59
ln (ab_T)	ln	9.09	+	0.81	*	ln (PGA)	0.44

Direct FE Method

Response [ln (S_d)]	PSDM						$\beta_{D\|PGA}$
	a			*b*			
ln (μ_φ)	ln	2.06	+	0.89	*	ln (PGA)	0.37
ln (fx_L)	ln	15.84	+	1.10	*	ln (PGA)	0.52
ln (fx_T)	ln	1.59	+	1.91	*	ln (PGA)	0.53
ln (ex_L)	ln	125.71	+	1.40	*	ln (PGA)	0.51
ln (ex_T)	ln	1.77	+	2.96	*	ln (PGA)	0.99
ln (ab_P)	ln	17.82	+	0.96	*	ln (PGA)	0.50
ln (ab_A)	ln	0.63	+	0.48	*	ln (PGA)	0.60
ln (ab_T)	ln	22.23	+	1.10	*	ln (PGA)	0.45

SOIL PROFILE #2 – No Liquefaction

Lumped Spring Method

Response [ln (S_d)]	PSDM						$\beta_{D\|PGA}$
	a			***b***			
ln (μ_φ)	ln	3.10	+	1.08	*	ln (PGA)	0.45
ln (fx_L)	ln	33.68	+	1.05	*	ln (PGA)	0.61
ln (fx_T)	ln	1.64	+	2.35	*	ln (PGA)	0.57
ln (ex_L)	ln	144.46	+	1.47	*	ln (PGA)	0.66
ln (ex_T)	ln	1.87	+	3.74	*	ln (PGA)	1.09
ln (ab_P)	ln	18.16	+	1.17	*	ln (PGA)	0.53
ln (ab_A)	ln	0.67	+	0.61	*	ln (PGA)	0.67
ln (ab_T)	ln	15.30	+	1.02	*	ln (PGA)	0.54

Winkler Spring Method

Response [ln (S_d)]	PSDM						$\beta_{D\|PGA}$
	a			***b***			
ln (μ_φ)	ln	2.72	+	1.05	*	ln (PGA)	0.43
ln (fx_L)	ln	26.73	+	1.17	*	ln (PGA)	0.63
ln (fx_T)	ln	1.72	+	2.26	*	ln (PGA)	0.59
ln (ex_L)	ln	123.10	+	1.46	*	ln (PGA)	0.65
ln (ex_T)	ln	1.96	+	3.59	*	ln (PGA)	1.12
ln (ab_P)	ln	19.07	+	1.13	*	ln (PGA)	0.55
ln (ab_A)	ln	0.70	+	0.59	*	ln (PGA)	0.69
ln (ab_T)	ln	10.21	+	0.91	*	ln (PGA)	0.49

Direct FE Method

Response [ln (S_d)]	PSDM						$\beta_{D\|PGA}$
	a			***b***			
ln (μ_φ)	ln	2.34	+	1.01	*	ln (PGA)	0.42
ln (fx_L)	ln	18.21	+	1.26	*	ln (PGA)	0.60
ln (fx_T)	ln	1.81	+	2.17	*	ln (PGA)	0.60
ln (ex_L)	ln	186.61	+	1.52	*	ln (PGA)	0.68
ln (ex_T)	ln	2.06	+	3.45	*	ln (PGA)	1.16
ln (ab_P)	ln	20.02	+	1.08	*	ln (PGA)	0.56
ln (ab_A)	ln	0.74	+	0.56	*	ln (PGA)	0.71
ln (ab_T)	ln	25.26	+	1.25	*	ln (PGA)	0.51

SOIL PROFILE #2 – Liquefaction

Lumped Spring Method

Response [ln (S_d)]	PSDM						$\beta_{D\|PGA}$
	a			*b*			
ln (μ_φ)	ln	4.34	+	1.51	*	ln (PGA)	0.63
ln (fx_L)	ln	45.47	+	1.42	*	ln (PGA)	0.82
ln (fx_T)	ln	2.25	+	3.22	*	ln (PGA)	0.78
ln (ex_L)	ln	212.30	+	1.45	*	ln (PGA)	0.78
ln (ex_T)	ln	2.54	+	5.09	*	ln (PGA)	1.48
ln (ab_P)	ln	24.33	+	1.57	*	ln (PGA)	0.71
ln (ab_A)	ln	0.89	+	0.81	*	ln (PGA)	0.89
ln (ab_T)	ln	21.42	+	1.43	*	ln (PGA)	0.76

Winkler Spring Method

Response [ln (S_d)]	PSDM						$\beta_{D\|PGA}$
	a			*b*			
ln (μ_φ)	ln	3.78	+	1.46	*	ln (PGA)	0.60
ln (fx_L)	ln	36.35	+	1.59	*	ln (PGA)	0.86
ln (fx_T)	ln	2.36	+	3.09	*	ln (PGA)	0.80
ln (ex_L)	ln	180.19	+	1.44	*	ln (PGA)	0.77
ln (ex_T)	ln	2.67	+	4.88	*	ln (PGA)	1.53
ln (ab_P)	ln	25.55	+	1.51	*	ln (PGA)	0.73
ln (ab_A)	ln	0.94	+	0.78	*	ln (PGA)	0.92
ln (ab_T)	ln	14.40	+	1.28	*	ln (PGA)	0.69

Direct FE Method

Response [ln (S_d)]	PSDM						$\beta_{D\|PGA}$
	a			*b*			
ln (μ_φ)	ln	3.14	+	1.35	*	ln (PGA)	0.56
ln (fx_L)	ln	25.13	+	1.74	*	ln (PGA)	0.83
ln (fx_T)	ln	2.48	+	2.97	*	ln (PGA)	0.83
ln (ex_L)	ln	262.96	+	1.41	*	ln (PGA)	0.75
ln (ex_T)	ln	2.80	+	4.69	*	ln (PGA)	1.57
ln (ab_P)	ln	26.83	+	1.45	*	ln (PGA)	0.75
ln (ab_A)	ln	0.98	+	0.75	*	ln (PGA)	0.95
ln (ab_T)	ln	35.11	+	1.74	*	ln (PGA)	0.71

APPENDIX D: FRAGILITY TABLES FOR THE BRIDGE COMPONENTS

SOIL PROFILE #1

Lumped Spring Method

Component	Slight		Moderate	
	med [IMm]	disp [βcomp]	med [IMm]	disp [βcomp]
Concrete Column [μϕ]	0.46	0.75	0.77	0.68
Fixed Bearing in Long. direction [fxL] (mm)	0.18	0.64	0.66	0.64
Rocker Bearing in Long. direction [exL] (mm)	0.39	0.65	1.00	0.63
Abutment-Transverse [abT] (mm)	0.70	0.94	3.17	1.13

Component	Extensive		Complete	
	med [IMm]	disp [βcomp]	med [IMm]	disp [βcomp]
Concrete Column [μϕ]	1.33	0.80	2.03	0.81
Fixed Bearing in Long. direction [fxL] (mm)	1.41	0.78	7.59	0.92
Rocker Bearing in Long. direction [exL] (mm)	1.22	0.64	1.55	0.68
Abutment-Transverse [abT] (mm)	7.00	1.08	N/A	N/A

Winkler Spring Method

Component	Slight		Moderate	
	med [IMm]	disp [βcomp]	med [IMm]	disp [βcomp]
Concrete Column [μϕ]	0.52	0.77	0.89	0.70
Fixed Bearing in Long. direction [fxL] (mm)	0.27	0.59	0.85	0.59
Rocker Bearing in Long. direction [exL] (mm)	0.52	0.60	1.16	0.58
Abutment-Transverse [abT] (mm)	1.10	1.02	5.83	1.23

Component	Extensive		Complete	
	med [IMm]	disp [βcomp]	med [IMm]	disp [βcomp]
Concrete Column [μϕ]	1.57	0.82	2.44	0.83
Fixed Bearing in Long. direction [fxL] (mm)	1.65	0.70	7.23	0.82
Rocker Bearing in Long. direction [exL] (mm)	1.37	0.60	1.67	0.62
Abutment-Transverse [abT] (mm)	14.04	1.18	N/A	N/A

Direct FE Method

Component	Slight		Moderate	
	med [IMm]	disp [βcomp]	med [IMm]	disp [βcomp]
Concrete Column [μϕ]	0.59	0.78	1.02	0.71
Fixed Bearing in Long. direction [fxL] (mm)	0.41	0.53	1.24	0.53
Rocker Bearing in Long. direction [exL] (mm)	0.35	0.56	0.87	0.54
Abutment-Transverse [abT] (mm)	0.47	0.76	1.62	0.91

Component	Extensive		Complete	
	med [IMm]	disp [βcomp]	med [IMm]	disp [βcomp]
Concrete Column [μϕ]	1.83	0.83	2.86	0.84
Fixed Bearing in Long. direction [fxL] (mm)	2.33	0.64	9.49	0.76
Rocker Bearing in Long. direction [exL] (mm)	1.06	0.56	1.33	0.59
Abutment-Transverse [abT] (mm)	3.10	0.87	N/A	N/A

SOIL PROFILE #2 – No Liquefaction

Lumped Spring Method

Component	Slight		Moderate	
	med [IMm]	disp [βcomp]	med [IMm]	disp [βcomp]
Concrete Column [μϕ]	0.44	0.69	0.70	0.63
Fixed Bearing in Long. direction [fxL] (mm)	0.19	0.63	0.61	0.63
Rocker Bearing in Long. direction [exL] (mm)	0.34	0.61	0.80	0.58
Abutment-Transverse [abT] (mm)	0.65	0.87	2.43	1.03

Component	Extensive		Complete	
	med [IMm]	disp [βcomp]	med [IMm]	disp [βcomp]
Concrete Column [μϕ]	1.12	0.72	1.63	0.73
Fixed Bearing in Long. direction [fxL] (mm)	1.18	0.73	5.11	0.85
Rocker Bearing in Long. direction [exL] (mm)	0.96	0.60	1.19	0.63
Abutment-Transverse [abT] (mm)	4.89	0.99	N/A	N/A

Winkler Spring Method

Component	Slight		Moderate	
	med [IMm]	disp [βcomp]	med [IMm]	disp [βcomp]
Concrete Column [μϕ]	0.49	0.70	0.78	0.64
Fixed Bearing in Long. direction [fxL] (mm)	0.28	0.58	0.78	0.58
Rocker Bearing in Long. direction [exL] (mm)	0.37	0.61	0.89	0.59
Abutment-Transverse [abT] (mm)	0.96	0.94	4.23	1.13

Component	Extensive		Complete	
	med [IMm]	disp [βcomp]	med [IMm]	disp [βcomp]
Concrete Column [μϕ]	1.28	0.73	1.87	0.74
Fixed Bearing in Long. direction [fxL] (mm)	1.41	0.67	5.26	0.77
Rocker Bearing in Long. direction [exL] (mm)	1.07	0.60	1.33	0.63
Abutment-Transverse [abT] (mm)	9.24	1.08	N/A	N/A

Direct FE Method

Component	Slight		Moderate	
	med [IMm]	disp [βcomp]	med [IMm]	disp [βcomp]
Concrete Column [μϕ]	0.55	0.72	0.90	0.65
Fixed Bearing in Long. direction [fxL] (mm)	0.41	0.52	1.08	0.52
Rocker Bearing in Long. direction [exL] (mm)	0.29	0.60	0.68	0.58
Abutment-Transverse [abT] (mm)	0.47	0.69	1.38	0.83

Component	Extensive		Complete	
	med [IMm]	disp [βcomp]	med [IMm]	disp [βcomp]
Concrete Column [μϕ]	1.50	0.76	2.22	0.77
Fixed Bearing in Long. direction [fxL] (mm)	1.87	0.60	6.34	0.70
Rocker Bearing in Long. direction [exL] (mm)	0.81	0.59	1.00	0.62
Abutment-Transverse [abT] (mm)	2.44	0.79	N/A	N/A

SOIL PROFILE #2 – Liquefaction

Lumped Spring Method

Component	Slight		Moderate	
	med [IMm]	disp [βcomp]	med [IMm]	disp [βcomp]
Concrete Column [μϕ]	0.45	0.57	0.62	0.54
Fixed Bearing in Long. direction [fxL] (mm)	0.24	0.61	0.56	0.61
Rocker Bearing in Long. direction [exL] (mm)	0.25	0.68	0.61	0.66
Abutment-Transverse [abT] (mm)	0.58	0.72	1.49	0.82

Component	Extensive		Complete	
	med [IMm]	disp [βcomp]	med [IMm]	disp [βcomp]
Concrete Column [μϕ]	0.87	0.59	1.13	0.60
Fixed Bearing in Long. direction [fxL] (mm)	0.91	0.67	2.71	0.74
Rocker Bearing in Long. direction [exL] (mm)	0.74	0.67	0.91	0.70
Abutment-Transverse [abT] (mm)	2.45	0.80	N/A	N/A

Winkler Spring Method

Component	Slight		Moderate	
	med [IMm]	disp [βcomp]	med [IMm]	disp [βcomp]
Concrete Column [μϕ]	0.48	0.58	0.67	0.54
Fixed Bearing in Long. direction [fxL] (mm)	0.32	0.56	0.69	0.56
Rocker Bearing in Long. direction [exL] (mm)	0.28	0.68	0.68	0.66
Abutment-Transverse [abT] (mm)	0.74	0.77	2.13	0.88

Component	Extensive		Complete	
	med [IMm]	disp [βcomp]	med [IMm]	disp [βcomp]
Concrete Column [μϕ]	0.95	0.60	1.25	0.61
Fixed Bearing in Long. direction [fxL] (mm)	1.06	0.61	2.80	0.68
Rocker Bearing in Long. direction [exL] (mm)	0.82	0.68	1.02	0.70
Abutment-Transverse [abT] (mm)	3.70	0.85	N/A	N/A

Direct FE Method

Component	Slight		Moderate	
	med [IMm]	disp [βcomp]	med [IMm]	disp [βcomp]
Concrete Column [μϕ]	0.52	0.60	0.74	0.56
Fixed Bearing in Long. direction [fxL] (mm)	0.44	0.50	0.88	0.50
Rocker Bearing in Long. direction [exL] (mm)	0.21	0.68	0.52	0.66
Abutment-Transverse [abT] (mm)	0.48	0.57	1.04	0.66

Component	Extensive		Complete	
	med [IMm]	disp [βcomp]	med [IMm]	disp [βcomp]
Concrete Column [μϕ]	1.09	0.63	1.46	0.64
Fixed Bearing in Long. direction [fxL] (mm)	1.31	0.55	3.17	0.61
Rocker Bearing in Long. direction [exL] (mm)	0.63	0.68	0.78	0.70
Abutment-Transverse [abT] (mm)	1.57	0.64	N/A	N/A

APPENDIX E: FRAGILITY TABLES FOR THE BRIDGE SYSTEM

Soil Profile #1

SSI Method	Slight		Moderate	
	med [IMm]	disp [βcomp]	med [IMm]	disp [βcomp]
Lumped Spring	0.32	0.70	0.71	0.66
Winkler Spring	0.39	0.68	0.87	0.64
Direct FE	0.50	0.66	1.13	0.62

SSI Method	Extensive		Complete	
	med [IMm]	disp [βcomp]	med [IMm]	disp [βcomp]
Lumped Spring	1.37	0.79	4.81	0.86
Winkler Spring	1.61	0.76	4.84	0.83
Direct FE	2.08	0.74	6.17	0.80

Soil Profile #2 – No liquefaction

SSI Method	Slight		Moderate	
	med [IMm]	disp [βcomp]	med [IMm]	disp [βcomp]
Lumped Spring	0.32	0.66	0.65	0.63
Winkler Spring	0.39	0.64	0.78	0.61
Direct FE	0.48	0.62	0.99	0.59

SSI Method	Extensive		Complete	
	med [IMm]	disp [βcomp]	med [IMm]	disp [βcomp]
Lumped Spring	1.15	0.73	3.37	0.79
Winkler Spring	1.34	0.70	3.57	0.76
Direct FE	1.68	0.68	4.28	0.73

Soil Profile #2 - Liquefaction

SSI Method	Slight		Moderate	
	med [IMm]	disp [βcomp]	med [IMm]	disp [βcomp]
Lumped Spring	0.34	0.59	0.59	0.57
Winkler Spring	0.40	0.57	0.68	0.55
Direct FE	0.48	0.55	0.81	0.53

SSI Method	Extensive		Complete	
	med [IMm]	disp [βcomp]	med [IMm]	disp [βcomp]
Lumped Spring	0.89	0.63	1.92	0.67
Winkler Spring	1.01	0.61	2.02	0.64
Direct FE	1.20	0.59	2.31	0.62